

Energetics of Inclusion-Induced Bilayer Deformations

Claus Nielsen,* Mark Goulian,# and Olaf S. Andersen*

*Department of Physiology and Biophysics, Cornell University Medical College, New York, New York 10021 and #Center for Studies in Physics and Biology, The Rockefeller University, New York, New York 10021 USA

ABSTRACT The material properties of lipid bilayers can affect membrane protein function whenever conformational changes in the membrane-spanning proteins perturb the structure of the surrounding bilayer. This coupling between the protein and the bilayer arises from hydrophobic interactions between the protein and the bilayer. We analyze the free energy cost associated with a hydrophobic mismatch, i.e., a difference between the length of the protein's hydrophobic exterior surface and the average thickness of the bilayer's hydrophobic core, using a (liquid-crystal) elastic model of bilayer deformations. The free energy of the deformation is described as the sum of three contributions: compression-expansion, splay-distortion, and surface tension. When evaluating the interdependence among the energy components, one modulus renormalizes the other: e.g., a change in the compression-expansion modulus affects not only the compression-expansion energy but also the splay-distortion energy. The surface tension contribution always is negligible in thin solvent-free bilayers. When evaluating the energy per unit distance (away from the inclusion), the splay-distortion component dominates close to the bilayer/inclusion boundary, whereas the compression-expansion component is more prominent further away from the boundary. Despite this complexity, the bilayer deformation energy in many cases can be described by a linear spring formalism. The results show that, for a protein embedded in a membrane with an initial hydrophobic mismatch of only 1 Å, an increase in hydrophobic mismatch to 1.3 Å can increase the Boltzmann factor (the equilibrium distribution for protein conformation) 10-fold due to the elastic properties of the bilayer.

INTRODUCTION

The hydrophobic membrane-spanning domains of integral membrane proteins (Singer and Nicolson, 1972) couple the proteins to the bilayer (Owicki et al., 1978). This hydrophobic coupling entails protein conformational changes possibly perturbing the structure of the surrounding bilayer. As a result, the free energy difference between two protein conformations will depend on the deformation energy associated with the bilayer perturbation. This provides a mechanism by which the lipid composition of the bilayer could play a role in determining protein conformation and protein function.

Numerous studies show that the function of integral membrane proteins is affected by bilayer lipid composition. Systematic investigations of this dependency of membrane protein function on the lipid bilayer composition show that chemical specificity is relatively unimportant for protein-lipid interactions (Devaux and Seigneuret, 1985; Bienvenüe and Marie, 1994). Rather, changes in membrane protein function can be correlated with changes in the bilayer material properties: bilayer hydrophobic thickness (Caffrey and Feigenson, 1981; Johannsson et al., 1981; Criado et al., 1984; Baldwin and Hubbell, 1985) and monolayer curvature stress (Brown, 1994; Navarro et al., 1984; McCallum and Epan, 1995). These effects are difficult to rationalize

within models that approximate the lipid bilayer as being equivalent to a thin sheet of liquid hydrocarbon, which is stabilized by the phospholipid polar groups.

Lipid bilayers, in fact, are self-assembled structures of amphipathic molecules with material properties similar to those of smectic liquid crystals (Helfrich, 1973; Evans and Hochmuth, 1978). Thus it is necessary to extend the liquid-hydrocarbon descriptions of the bilayer to incorporate the bilayer curvature component of the deformation energy (Canham, 1970; Helfrich, 1973; Brochard and Lennon, 1975; Brochard et al., 1976), changes in bilayer thickness and the associated compressibility modulus (Evans and Hochmuth, 1978; Mouritsen and Bloom, 1984; Bloom et al., 1991), and changes in bilayer surface area and the associated interfacial tension (Abney and Owicki, 1985; Marcelja, 1976; Owicki and McConnell, 1979).

The theory of liquid crystal elastic deformations (Helfrich, 1973), which provides for a coherent continuum description of the shapes of lipid vesicles, can be used to describe free energy differences associated with membrane perturbations due to protein-bilayer interactions (Huang, 1986; Helfrich and Jakobsson, 1990; Dan et al., 1993, 1994; Ring, 1996). In this description the curvature component is associated with the monolayer curvature and is a local parameter, i.e., only dependent upon the conditions at bilayer/inclusion boundary. Global curvature contributions reflecting intrinsic asymmetry between the inner and outer monolayer, which give rise to an area difference elasticity term (e.g., Miao et al., 1994), are not considered.

The model analyzed in this paper emphasizes the coupling between a bilayer and its embedded proteins (inclusions) in terms of membrane mechanics and energetics that provides for a thermodynamically based description of lip-

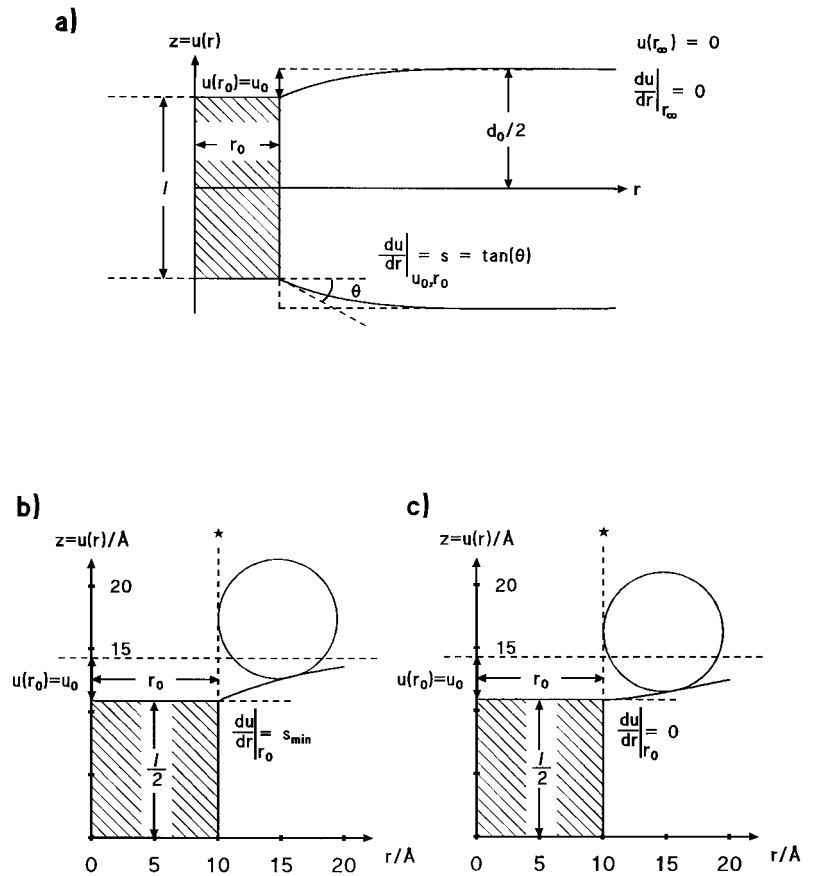
Received for publication 14 October 1997 and in final form 29 December 1997.

Address reprint requests to Claus Nielsen, Department of Physiology and Biophysics, Cornell University Medical College, 1300 York Avenue, Rm C-514, New York, NY 10021. Tel.: (212) 746-6351; Fax: (212) 746-8690; E-mail: cnielsen@mail.med.cornell.edu.

© 1998 by the Biophysical Society

0006-3495/98/04/1966/18 \$2.00

FIGURE 1 The model. (a) The total deformation free energy is determined by the bilayer deformation profile associated with a hydrophobic mismatch between the bilayer and the inclusion. The inclusion is treated as a rotationally symmetrical deformation of the bilayer. Assuming midplane symmetry (a symmetrical bilayer), the problem can be reduced to a radially varying deformation of a monolayer with unperturbed thickness $d_0/2$, where $u(r)$ denotes the local perturbation in monolayer thickness at the distance r from the luminal axis. At the channel-bilayer contact surface, r_0 , the deformation is u_0 . The first derivative at the contact surface (the contact slope) du/dr is s . (b and c) The two different boundary conditions considered. Bilayer deformation profiles are drawn to scale. The circles represent the polar headgroup for a phosphatidylcholine lipid molecule, the vertical dotted lines marked by asterisks denote integration limits. In (b) $s = s_{\min}$ and in (c) $s = 0$. The deformation profiles obtained using the elastic membrane model define the average hydrocarbon/headgroup boundary. The actual (instantaneous) profile will be less well-defined due to thermal motion of the bilayer lipids perpendicular to the bilayer/solution interface (Wiener and White, 1992).



id-protein interactions. The purpose of the present article is to examine some generic consequences of such a liquid crystal theory-based model of bilayer deformation energy. The results demonstrate that the bilayer deformation energy can be as large as 10–15 kJ/mol—comparable with effects of point mutations on protein function—indicating that bilayer material properties can play an equally important role in protein function. Some of the results have appeared in preliminary form (Nielsen et al., 1997).

THEORY

The model

A length mismatch between the bilayer hydrophobic core and the hydrophobic exterior surface of a membrane inclusion (integral membrane protein) will perturb the lipid packing in the vicinity of the inclusion (Fig. 1). Following Huang (1986) we approximate the changes in lipid packing as occurring in three independent modes or components: compression-expansion (CE, due to changes in bilayer thickness) with a characteristic elastic deformation modulus K_a ; splay-distortion (SD, due to variation in the director among adjacent lipid molecules) with a splay-distortion modulus K_c ; and surface tension (ST, due to changes in bilayer surface area) with interfacial tension α . The magnitude of each energy component will vary with the magni-

tude of the corresponding modulus and, as we will see later, vary as a function of the other moduli.

For a given set of moduli the shape of the bilayer deformation will be one that minimizes the total free energy cost of the deformation. Assuming that the three components splay-distortion, compression-expansion, and surface tension are sufficient to describe the problem,¹ the deformation free energy ΔG_{def} for the situation shown in Fig. 1 a can be described (to second order) as the surface integral

$$\Delta G_{\text{def}} = \int_{\Omega} \frac{1}{2} \left\{ \frac{K_a}{d_0^2} u^2 + K_c \left(\frac{\partial^2 u}{\partial x^2} + \frac{\partial^2 u}{\partial y^2} - C_0 \right)^2 + \alpha \left[\left(\frac{\partial u}{\partial x} \right)^2 + \left(\frac{\partial u}{\partial y} \right)^2 \right] \right\} d\Omega \quad (1)$$

where d_0 is the bilayer equilibrium thickness, $u(x, y)$ the local monolayer perturbation, and C_0 is the spontaneous monolayer curvature. In the following we take $C_0 = 0$.

¹One also may have an energy contribution proportional to the degree of tilt of lipid molecules—a situation where the lipid molecule director is not aligned with its corresponding surface normal (Helfrich, 1973). Also, strong hydrophobic coupling may fail for larger bilayer deformations.

To determine the minimum free energy conformation, the integral in Eq. 1 is minimized with respect to variations in $u(x, y)$. In Cartesian coordinates

$$\Delta G_{\text{def}} = \int_a^b \int_c^d \psi \left(x, y, u, \frac{\partial u}{\partial x}, \frac{\partial u}{\partial y}, \frac{\partial^2 u}{\partial x^2}, \frac{\partial^2 u}{\partial y^2} \right) dx dy \quad (2)$$

and one determines the function $u = f(x, y)$ that minimizes the integral by calculating the variation of the integral in Eq. 2 (Lebedev et al., 1979). The variation integral vanishes for arbitrary variations δu if $u = f(x, y)$ is a solution of Lagrange's equation:

$$\begin{aligned} \frac{\partial \psi}{\partial u} - \frac{\partial}{\partial x} \left(\frac{\partial \psi}{\partial (\partial u / \partial x)} \right) - \frac{\partial}{\partial y} \left(\frac{\partial \psi}{\partial (\partial u / \partial y)} \right) \\ + \frac{\partial^2}{\partial x^2} \left(\frac{\partial \psi}{\partial (\partial^2 u / \partial x^2)} \right) + \frac{\partial^2}{\partial y^2} \left(\frac{\partial \psi}{\partial (\partial^2 u / \partial y^2)} \right) = 0 \end{aligned} \quad (3)$$

Substituting Eq. 1 into Eq. 3 leads to the linear differential equation

$$K_c \nabla^4 u - \alpha \nabla^2 u + \left(\frac{K_a}{d_0^2} \right) u = 0,$$

where (4)

$$\nabla^2 = \frac{\partial^2}{\partial x^2} + \frac{\partial^2}{\partial y^2}$$

Four boundary conditions are needed to solve Eq. 4 (see Fig. 1 *a*). Three of these are straightforward. Using radial symmetry (with $r = \sqrt{x^2 + y^2}$), for $r \rightarrow \infty$, the bilayer perturbation will approach zero. We thus have the following two conditions:

$$u(r_\infty) = 0, \quad (5a)$$

$$\left. \frac{du}{dr} \right|_{r_\infty} = 0. \quad (5b)$$

A third boundary condition arises from the hydrophobic coupling between the hydrophobic core of the bilayer and the hydrophobic exterior surface of the embedded inclusion at the bilayer/inclusion contact surface, which determines the deformation at the bilayer/inclusion boundary:

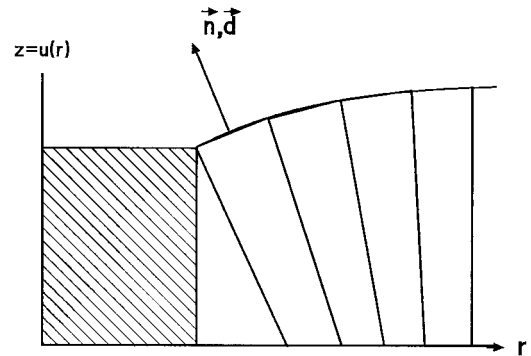
$$u(r_0) = u_0 = (d_0 - l)/2 \quad (5c)$$

Eq. 5c is valid only in the limit of strong hydrophobic coupling, i.e., the case where the strength of the interaction is such that there is no exposure of hydrophobic residues to water.

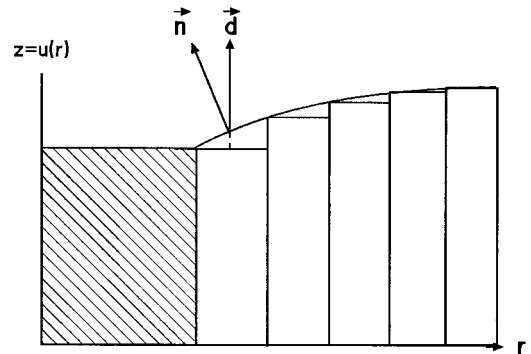
The fourth boundary condition has been formulated in several different ways (Huang, 1986; Helfrich and Jakobsson, 1990; Dan et al., 1993, 1994; Ring, 1996). Helfrich and Jakobsson (1990) proposed that $du/dr|_{r_0} = s_{\text{min}}$ the value of the contact slope s for which G_{def} is minimized (Fig. 1 *b*). This "free" boundary condition implies that $(\partial/\partial r)\nabla^2 u|_{r_0} = 0$ (cf. Landau and Lifshitz, 1986, p. 44). Physically, the free

boundary condition implies that the lipid molecules are allowed some degree of tilt (Fig. 2, *a* and *b*). Huang (1986) used experimental results, namely the variation of gramicidin channel lifetime as a function of bilayer thickness, to evaluate the contact slope. The analysis showed that the slope was zero or close to zero (Fig. 1 *c*), a result that differs considerably from $(\partial/\partial r)\nabla^2 u|_{r_0} = 0$. This can be rationalized by assuming that the tilt of lipid molecules is associated

a)



b)



c)

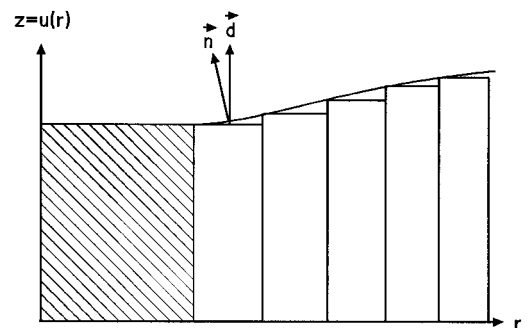


FIGURE 2 Lipid packing close to the inclusion. (*a*) Situation with no lipid molecule tilt and $s < 0$. The molecule director \vec{d} is parallel to the surface normal \vec{n} at every point. This hypothetical situation will create a void at the inclusion-bilayer boundary. (*b*) When the first lipid molecule is forced to be closely aligned at the boundary for $s < 0$ implies that the molecule director cannot align with the corresponding surface normal, i.e., the molecules are tilted. (*c*) When there is close alignment at the boundary, the need for lipid molecule tilt will be diminished with the $s = 0$ condition (in the case of cylindrical inclusions).

with a significant energetic penalty (see Fig. 2 c), as previously discussed by Helfrich (1973).

To partially account for the ensuing uncertainties we investigate two different boundary conditions: a free contact slope and a clamped contact slope

$$\left. \frac{\partial}{\partial r} \nabla^2 u \right|_{r_0} = 0 \quad (s = s_{\min}) \quad (5d)$$

$$\left. \frac{\partial u}{\partial r} \right|_{r_0} = s. \quad (5e)$$

We cannot exclude that more elaborate boundary conditions should be used, but they would require more parameters than can be justified when using a second-order continuum approximation (Eq. 1). In Appendix I we examine a specific set of boundary conditions that were proposed by Ring (1996) and show how they reduce to Eq. 5d.

Solution

The Euler-Lagrange equation, Eq. 4, can be rewritten as

$$\nabla^4 u - \gamma \nabla^2 u + \beta u = 0 \quad (6)$$

where

$$\gamma = \frac{\alpha}{K_c} \quad \beta = \frac{K_a}{d_0^2 K_c} \quad (7)$$

Solutions of Eq. 6 that vanish for $r \rightarrow \infty$ can be expressed as a linear combination of modified zero-order Bessel functions of the second kind (see Appendix II) which satisfy

$$\nabla^2 \mathcal{H}_0(kr) = k^2 \mathcal{H}_0(kr) \quad (8)$$

We therefore have

$$k^4 - \gamma k^2 + \beta = 0 \Rightarrow k_{\pm}^2 = \frac{\gamma \pm \sqrt{\gamma^2 - 4\beta}}{2}, \quad (9)$$

and $u(r)$ can be written as

$$u(r) = A_+ \mathcal{H}_0(k_+ r) + A_- \mathcal{H}_0(k_- r) \quad (10)$$

The boundary conditions at the bilayer/inclusion boundary (for clamped contact slope) provide the constraints:

$$u(r_0) = u_0 \Rightarrow A_+ \mathcal{H}_0(k_+ r_0) + A_- \mathcal{H}_0(k_- r_0) = u_0 \quad (11a)$$

and (for a fixed s)

$$u'(r_0) = s \Rightarrow A_+ k_+ \mathcal{H}_1(k_+ r_0) + A_- k_- \mathcal{H}_1(k_- r_0) = -s \quad (11b)$$

where \mathcal{H}_1 is the modified first-order Bessel function of the second kind (Abramowitz and Stegun, 1968). The coefficients A_{\pm} are

$$A_+ = \frac{k_- \mathcal{H}_1(k_- r_0) u_0 + \mathcal{H}_0(k_- r_0) s}{k_- \mathcal{H}_0(k_+ r_0) \mathcal{H}_1(k_- r_0) - k_+ \mathcal{H}_0(k_- r_0) \mathcal{H}_1(k_+ r_0)} \quad (12a)$$

$$A_- = \frac{-k_+ \mathcal{H}_1(k_+ r_0) u_0 - \mathcal{H}_0(k_+ r_0) s}{k_- \mathcal{H}_0(k_+ r_0) \mathcal{H}_1(k_- r_0) - k_+ \mathcal{H}_0(k_- r_0) \mathcal{H}_1(k_+ r_0)} \quad (12b)$$

and the expression for the deformation free energy becomes (see Appendix II)

$$\Delta G_{\text{def}} = -\pi r_0 K_c [s(A_+ k_+^2 \mathcal{H}_0(k_+ r_0) + A_- k_-^2 \mathcal{H}_0(k_- r_0)) + u_0(A_+ k_+^3 \mathcal{H}_1(k_+ r_0) + A_- k_-^3 \mathcal{H}_1(k_- r_0)) + \gamma u_0 s] \quad (13)$$

To investigate the interdependence between specific energy contributions we solved the Euler-Lagrange equation numerically. To do so, Eq. 4 is expressed as

$$K_c \left(\frac{1}{r^3} \frac{du}{dr} - \frac{1}{r^2} \frac{d^2 u}{dr^2} + \frac{2}{r} \frac{d^3 u}{dr^3} + \frac{d^4 u}{dr^4} \right) - \alpha \left(\frac{1}{r} \frac{du}{dr} + \frac{d^2 u}{dr^2} \right) + \frac{K_a}{d_0^2} u = 0 \quad (14)$$

The total deformation free energy integral Eq. 1 can also be expressed in cylindrical coordinates:

$$\Delta G_{\text{def}} = \pi \int_{r_0}^{r_{\infty}} \left[\frac{K_a}{d_0^2} u^2 + K_c \left(\frac{1}{r} \frac{du}{dr} + \frac{d^2 u}{dr^2} \right)^2 + \alpha \left(\frac{du}{dr} \right)^2 \right] r dr \quad (15)$$

where the energy component corresponding to the compression-expansion modulus can be identified as

$$\Delta G_{\text{CE}} = \pi \int_{r_0}^{r_{\infty}} \frac{K_a}{d_0^2} u^2 r dr, \quad (16a)$$

the energy component corresponding to the splay-distortion modulus as

$$\Delta G_{\text{SD}} = \pi \int_{r_0}^{r_{\infty}} \left[K_c \left(\frac{1}{r} \frac{du}{dr} + \frac{d^2 u}{dr^2} \right)^2 \right] r dr, \quad (16b)$$

and the energy component corresponding to the surface tension modulus as

$$\Delta G_{\text{ST}} = \pi \int_{r_0}^{r_{\infty}} \alpha \left(\frac{du}{dr} \right)^2 r dr \quad (16c)$$

For the energy decomposition we solved Eqs. 14–16 numerically as a two-point boundary value problem using standard relaxation methods (Press et al., 1986).

Parameters

To facilitate comparison with previous studies (Huang, 1986; Helfrich and Jakobsson, 1990), our reference system is a thin, solvent-free lipid bilayer with an embedded inclusion that has dimensions similar to those of a gramicidin channel (see Fig. 1 a and Tables 1 and 2). The standard parameter set used by Huang (1986) and Helfrich and Jakobsson (1990), which is listed in Table 2, defines this reference membrane. These parameter values are identified by asterisks in the following.

TABLE 1 List of symbols

Symbol	Meaning	Unit
u	Monolayer perturbation	\AA
r	Radial distance from inclusion symmetry axis	\AA
d_0	Unperturbed bilayer thickness	\AA
l	Hydrophobic length of inclusion	\AA
u_0	Monolayer deformation at inclusion-bilayer boundary	\AA
r_0	r at inclusion-bilayer boundary = radius of inclusion	\AA
r_∞	Radial distance limit where $u(r) = 0$	\AA
s	Contact slope at inclusion-bilayer boundary	—
C_0	Spontaneous monolayer curvature	\AA^{-1}
K_a	Area compression-expansion modulus	$N/\text{\AA}^2$
\bar{B}	Volume compression-expansion modulus	$N/\text{\AA}^2$
K_c	Splay-distortion modulus (dimensions of energy)	$N/\text{\AA}$
K_1	Splay-distortion modulus (dimensions of force)	$N/\text{\AA}$
α	Bulk interfacial surface tension	$N/\text{\AA}$
σ	Bilayer interfacial surface tension	$N/\text{\AA}$
ΔG_{def}	Total deformation free energy	kT
ΔG_{CE}	Nominal compression-expansion energy component	kT
ΔG_{SD}	Nominal splay-distortion energy component	kT
ΔG_{ST}	Nominal surface tension energy component	kT
$\beta^{-1/4}$	Characteristic length scale = $\sqrt{\xi d_0}$	\AA
H	Phenomenological spring constant	$\text{kT}/\text{\AA}^{-2}$
ρ_a	Radial distance from r_0 beyond which $ u < u_0/e $	\AA
ρ_a	Radial distance from r_0 within which one has $(1 - 1/e)$ of ΔG_{def}	\AA
μ	Exponent for K_c dependence ($\Delta G \sim K_c^\mu$ or $H \sim K_c^\mu$)	—
ν	Exponent for K_a dependence ($\Delta G \sim K_a^\nu$ or $H \sim K_a^\nu$)	—
δ	Exponent for r_0 dependence ($\Delta G \sim r_0^\delta$ or $H \sim r_0^\delta$)	—

There is, however, uncertainty about what would be the “correct” value for any of the material constants. First, the measured parameters are macroscopic entities whereas the quantities in Eq. 1 reflect the microscopic behavior close to the inclusion; there may not be exact correspondence between the two classes. Second, the measured parameters are not unique in the sense that different experimental methods have provided different values for a given parameter (cf. Niggemann et al., 1995); even more importantly, the material properties vary as a function of membrane composition.

Pipette aspiration methods [for reviews see Evans and Needham (1987) and Needham, (1995)] have been used to obtain area compression-expansion values K_a that range from $5.7 \cdot 10^{-12} N/\text{\AA}$ for diarachidonylphosphatidylcholine (DAPC) bilayers to $1.9 \cdot 10^{-11} N/\text{\AA}$ in 1-stearoyl-2-oleoyl-

phosphatidylcholine (SOPC) bilayers.² The modulus increases with increasing cholesterol mole fraction: from $2.6 \cdot 10^{-11} N/\text{\AA}$ in SOPC bilayers with 14 mol % cholesterol to $1.2 \cdot 10^{-10} N/\text{\AA}$ in SOPC bilayers with 58 mol % cholesterol (Needham and Nunn, 1990). Given this variability, we investigate the behavior of the model over two decades in K_a centered around the reference value.

The splay-distortion modulus K_c (dimensions of energy) is expected to be $10^{-19} J$, as estimated from elastic energy densities in vesicles approximated as a sum of nearest-neighbor contributions (Helfrich, 1973). This estimate is remarkably close to the experimental value obtained by Evans and Rawicz (1990) for SOPC bilayers using measurements based on thermal fluctuations. They found $K_c = 9 \cdot 10^{-20} J$; the corresponding value for DAPC bilayers was $4.4 \cdot 10^{-20} J$. Addition of cholesterol to the bilayer increases the elastic bending modulus threefold: $K_c = 2.5 \cdot 10^{-19} J$ for SOPC bilayers with 50 mol % cholesterol (Evans and Rawicz, 1990). Using a different technique (tether formation from giant lipid vesicles) Song and Waugh (1993) found comparable values for SOPC bilayers: $K_c = 1.2 \cdot 10^{-19} J$, and for SOPC bilayers with 50 mol % cholesterol, $K_c = 3.3 \cdot 10^{-19} J$, in good agreement with the threefold increase observed by Evans and Rawicz (1990). Our standard parameter set has a rather low value for $K_c^* = 2.85 \cdot 10^{-20} J$, but we investigate the behavior of the model for a range of values up to $10 \cdot K_c^*$ corresponding to the elastic bending modulus for cholesterol-containing bilayers.³

The surface tension in a monolayer spread at an air/water interface has a finite value which is $\sim 3 \cdot 10^{-12} N/\text{\AA}$ (Nagle, 1980): that of a hydrocarbon/air interface. For bilayers with zero local and global curvature—giant vesicular membranes in osmotic equilibrium, for example—the situation is different. The unperturbed bilayer will, under these circumstances, adopt a state in which the attractive interactions in the hydrophobic chains and the interfacial region balance the repulsive interactions between the headgroups (Seddon, 1990). In this case the free energy is minimal with respect to the area of the membrane; that is, the derivative of the free energy with respect to area vanishes, the result being a state of optimal packing of the lipid molecules, i.e., a bilayer

TABLE 2 Reference parameters

Symbol	Value	Unit	Reference
d_0	28.5	\AA	Elliott et al., 1983
l	21.7	\AA	Elliott et al., 1985
u_0	3.40	\AA	$(d - l)/2$
r_0	10	\AA	Hendry et al., 1978
C_0	0	\AA^{-1}	—
K_c^*	$2.85 \cdot 10^{-10}$	$N/\text{\AA}$	Helfrich, 1973; Schneider et al., 1984; Engelhart et al., 1985 ($K_c = d_0 K_1$)
K_a^*	$1.425 \cdot 10^{-11}$	$N/\text{\AA}$	White, 1978; Hladky and Gruen, 1982 ($K_a = d_0 \bar{B}$)
α^*	$3 \cdot 10^{-13}$	$N/\text{\AA}$	Elliott and Haydon, 1979

²The area compression-expansion modulus K_a can also be determined from the volume compression-expansion modulus \bar{B} as $K_a = d_0 \bar{B}$. Bilayer capacitance measurements (White, 1978), although indirect, allow for comparison between glycerolmonooleate (GMO) bilayers and phospholipid bilayers. Using this method Hladky and Gruen (1982) estimated that $\bar{B} = 5 \cdot 10^{-13} N/\text{\AA}^2$ for nominally solvent-free GMO bilayers (formed with squalene). Alvarez and Latorre (1978) estimated that $\bar{B} = 8 \cdot 10^{-13} N/\text{\AA}^2$ for nominally solvent-free GMO membranes formed using pentane and $1.3 \cdot 10^{-12} N/\text{\AA}^2$ for nominally solvent-free bacterial phosphatidylethanolamine bilayers. For our reference bilayer thickness d_0 the corresponding K_a values range from $1.4 \cdot 10^{-11} N/\text{\AA}$ to $3.7 \cdot 10^{-11} N/\text{\AA}$.

³In liquid crystals the splay-distortion modulus sometimes is determined as a force, denoted by K_1 ($= K_c/d_0$). K_1 has been estimated to be $2 \cdot 10^{-11} N$ when the lamellar repeat distance was 60\AA , and $1 \cdot 10^{-11} N$ when lamellar repeat was 20\AA , which corresponds to $K_c = 2 \cdot 10^{-20} J$ (de Gennes, 1974).

where the interfacial bilayer surface tension σ vanishes (Jähnig, 1996).

For bilayers surrounded by a Plateau-Gibbs border the difference between the interfacial bilayer surface tension σ and the bulk interfacial tension α of the Plateau-Gibbs border is finite, reflecting the free energy of thinning the bilayer. Under these experimental conditions α can be determined using the Lippmann equation (Requena and Haydon, 1975), and for GMO/squalene membranes, $\alpha = 3 \cdot 10^{-13} \text{ N/\AA}$ (Elliott and Haydon, 1979). For phosphatidylcholine/*n*-decane bilayers α vary between $1.6 \cdot 10^{-13} \text{ N/\AA}$ and $4.8 \cdot 10^{-13} \text{ N/\AA}$ (Neher and Eibl, 1977; Requena and Haydon, 1975).

In the following we will consider a solvent-free membrane with zero local and global curvature (i.e., $\sigma = 0$) and use the GMO/squalene value as our reference parameter for the bulk interfacial surface tension α .

RESULTS

Choice of boundary conditions

The bilayer deformation energy varies as a function of mechanical moduli as well as the boundary conditions at $r = r_0$. Fig. 3 *a* shows (analytical and numerical) solutions to Eq. 4 as a function of s for the reference membrane (Table 2). The results agree with those of Helfrich and Jakobsson (1990). The energy is at a minimum when $s = -0.446$, in which case $\Delta G_{\text{def}}^* = 4.05 \text{ kT}$. This solution does not, however, consider the energetic cost associated with the packing of the lipid molecules immediately adjacent to the inclusion. This could be a problem because lipid molecules cannot just sway away from the inclusion, as this would create a void at the inclusion/acyl chain boundary (Fig. 2 *a*). The $s = s_{\text{min}}$ boundary condition therefore implies that the acyl chains are allowed to tilt, meaning that the lipid molecule director is not parallel to the membrane normal (see Fig. 2 *b*).

If the penalty for tilt is high, then for cylindrical inclusions (Fig. 2 *c*), the headgroups of the lipid molecules in the concentric annuli surrounding the inclusion will be nearly in the same z plane, which corresponds to a situation where $s = 0$. In this case, the deformation energy will differ considerably from the results obtained when $s = s_{\text{min}}$ (see Fig. 3 *b*).

The two curves in Fig. 3 *b* represent solutions of Eq. 14 for the boundary conditions Eqs. 5 *d* and 5 *e*, respectively. The curve labeled (1): $s = s_{\text{min}}$ shows the deformation energy versus u_0 for the $s = s_{\text{min}}$ boundary condition (i.e., the value of 4.05 kT for ΔG_{def} at $u_0^* = 3.4 \text{ \AA}$ in Fig. 3 *b* corresponds to the minimum in the curve shown in Fig. 2 *a*). The curve labeled (2): $s = 0$ represents a solution similar to that obtained by Huang (1986) with much larger deformation energies ($\Delta G_{\text{def}} = 11.86 \text{ kT}$ for $u_0^* = 3.4 \text{ \AA}$) than the $s = s_{\text{min}}$ solution. In both cases ($s = s_{\text{min}}$ and $s = 0$) we assume strong hydrophobic coupling between inclusion and

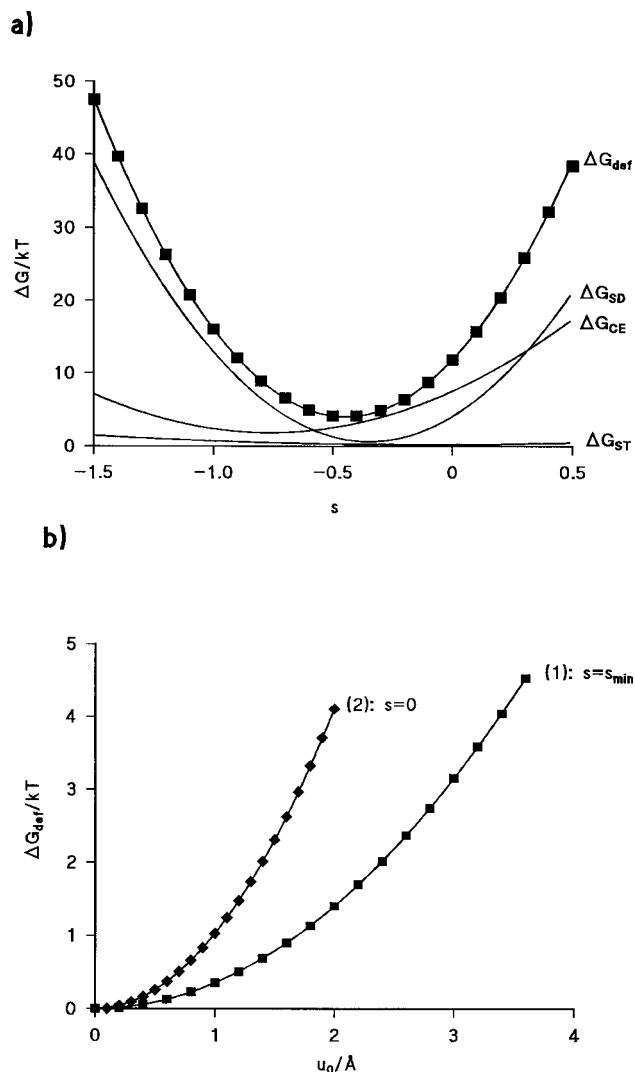


FIGURE 3 (a) The deformation free energy associated with insertion of an inclusion with dimensions of a gramicidin dimer channel in a lipid bilayer. Parameters were as listed in Table 2. The energy components for splay-distortion (ΔG_{SD}), compression-expansion (ΔG_{CE}), and surface tension (ΔG_{ST}) are indicated. The analytical solution (Eq. 13) for specific values of s is indicated by solid squares; the lines represent numerical solutions to Eq. 15 and Eq. 16a–c. (b) Comparison of different solutions to the deformation energy problem. The deformation u_0 is varied in steps of 0.2 \AA , and the corresponding values for ΔG_{def} are connected by lines. Otherwise, reference parameters (Table 2). (1) ΔG_{def} for the case where the contact slope is determined by the minimum energy constraint, $s = s_{\text{min}}$ (Fig. 1 *b*). (2) ΔG_{def} for the case of $s = 0$ (Fig. 1 *c*).

the first annulus of surrounding lipid molecules [$u_0 = (d_0 - l)/2$], meaning that the vertical position of the lipid molecules is determined completely by the hydrophobic part of the inclusion.

The bilayer deformation profile

The shape of the deformation profile varies as a function of the elastic moduli. Using Eq. 4 we find that the surface

tension component (ΔG_{ST}) can be neglected provided that

$$\alpha \ll \sqrt{\frac{K_a K_c}{d_0^2}}, \quad (17)$$

as is the case for the reference membrane. In this case there is only a single length scale in the free energy expression (cf. Eq. 1). It is convenient to characterize the deformation profile using the length scale

$$(K_c d_0^2 / K_a)^{1/4} = \beta^{-1/4} = \sqrt{\xi d_0}, \quad (18)$$

where $\xi = \sqrt{K_c / K_a}$ (see Eqs. 7–10 and Appendix II). For a given d_0 , the deformation energy (and profile, see below) are functions of the ratio K_c / K_a and K_a (or K_c). We now examine some consequences of this.

Depending on the value of s , the bilayer deformation profile may be nonmonotonic. That is, the energy minimization requirement may cause a bilayer compression adjacent to the inclusion to induce an expansion further away from the bilayer/inclusion boundary. Such shapes arise because the deformation profile is determined by the need to minimize of the overall deformation energy, which has implications for lipid packing. The packing problem arises because the hydrophobic core volume per unit bilayer surface will deviate from its equilibrium value. As K_a increases (for a constant K_c), the ΔG_{CE} component of ΔG_{def} will tend to increase, which is reflected in the shape of the deformation: the deformation will be localized close to the inclusion as splay-distortion becomes relatively inexpensive (in terms of energy) and the minimization will primarily affect ΔG_{CE} . As K_c increases (for a constant K_a), ΔG_{SD} will tend to increase, which leads to “long-range” deformations (minimization will primarily affect ΔG_{SD} at the cost of increasing compression-expansion). This is illustrated in Fig. 4 and Table 3.

The profiles shown in Fig. 4 illustrate the bilayer deformation for different choices of parameters and for three different choices of s . Fig. 4, *a–c* was generated with the reference parameters ($\beta^{*-1/4} = 11.3 \text{ \AA}$); Fig. 4, *d–f* was generated using $K_a = 0.01 K_a^*$, which corresponds to a “soft” bilayer ($\beta^{-1/4} = 35.7 \text{ \AA}$). When describing the bilayer deformations it is helpful to introduce a characteristic deformation length $\rho_u = r_{1/e} - r_0$, where $|u(r_{1/e})| = u_0/e$ and e is the base of the natural logarithm. In case of nonmonotonic deformations, where ρ_u may be a multivalued function, we define ρ_u to be the maximal functional value. A characteristic energy length ($\rho_{\Delta G}$) can be defined similarly, as the distance $\rho_{\Delta G} = r_{\Delta G} - r_0$, where $r_{\Delta G}$ is the radius within which one has $(1 - 1/e)$ of the total energy ΔG_{def} :

$$\pi \int_{r_0}^{r_0 + \rho_{\Delta G}} \left[\frac{K_a}{d_0^2} u^2 + K_c \left(\frac{1}{r} \frac{du}{dr} + \frac{d^2 u}{dr^2} \right)^2 + \alpha \left(\frac{du}{dr} \right)^2 \right] r dr \quad (19)$$

$$= (1 - 1/e) \Delta G_{def}$$

The selected ρ criteria for deformation and energy distribution are arbitrary. With a 10% criterion instead of a 1/e

criterion the absolute values for ρ_u and $\rho_{\Delta G}$ will be different, but the qualitative trends are unchanged (results not shown).

In Fig. 4 *a*, $s = -1$, the bilayer expansion is small, and the maximal expansion is less than u_0/e , which results in a small value for ρ_u . Fig. 4 *d* shows the same situation but for a “softer” bilayer (a bilayer with a larger K_c/K_a or $\beta^{-1/4}$). In this case the maximal expansion is greater than u_0/e , and ρ_u is not a single-valued function of $u(r)$, which results in a higher value for ρ_u . The ΔG_{ST} contribution to ΔG_{def} increases twofold, and its relative importance becomes more pronounced: ΔG_{ST} is 5% of ΔG_{def} in the reference membrane, but increases to 18% of ΔG_{def} in the softest bilayer (see Table 3).

In the second pair of profiles (Fig. 4, *b* and *e*) $s = -0.5$, which is close to s_{min} . Both profiles display maximal bilayer expansions less than u_0/e . An increase in bilayer “softness” by a factor of 100 (Fig. 4 *e*) does not significantly affect ρ_u , and the shape of the deformation profile is fairly similar in these two situations. Several features of the energy decomposition are noteworthy, however. First, the absolute ΔG_{CE} contribution to ΔG_{def} decreases almost 30-fold when K_a changes from K_a^* to $0.01 K_a^*$, whereas ΔG_{SD} decreases only twofold. Second, in the reference (“hard”) bilayer the relative contributions of ΔG_{SD} and ΔG_{CE} are inverted as one goes from $s = -1$ to $s = -0.5$, which is not the case for the softer bilayer. Third, ΔG_{ST} is a larger component (29%) of ΔG_{def} in the softest bilayer as compared to the reference bilayer (8%).

Finally, the third pair of profiles (Fig. 4, *c* and *f*) when $s = 0$ shows an example of monotonic deformations. For the soft bilayer $\Delta G_{CE} > \Delta G_{SD}$, which is not the case for the reference bilayer (see Fig. 3 *a*). Hence the need to minimize the compression-expansion component is less, and the bilayer primarily minimizes the ΔG_{SD} component, which results in long-range (i.e., several times the bilayer thickness) deformations (see Fig. 4 *f*).

To get further insight into how the system responds to the choice of boundary conditions it is helpful to examine how ρ_u and $\rho_{\Delta G}$ vary as a function of s for different values of K_a . This is shown in Fig. 5. The different values for K_a correspond to different values of $\beta^{-1/4}$, because K_c is kept constant. For softer bilayers [curves 2 ($\beta^{-1/4} = 20.1 \text{ \AA}$) and 3 ($\beta^{-1/4} = 35.7 \text{ \AA}$)] and negative s , ρ_u increases markedly with decreasing s because of a bilayer expansion close to the bilayer/inclusion contact surface (Fig. 4 *d*). A continuous change in s , going from $s = -1$ (Fig. 4 *b*) to $s = -0.5$ (Fig. 4 *d*), causes a discontinuous change in ρ_u reflecting the nonmonotonic deformation (the jumps in curves 2 and 3 in Fig. 5 *a*).⁴ For $s \approx -0.5$, the deformation extension length and the total free energy of deformation are decoupled: variations in $\beta^{-1/4}$, due to changes in K_a , produce no change in the radial extent of deformation when measured by ρ_u (cf. Fig. 4, *b* and *e*), but the absolute energies change (from 4.05

⁴The reference membrane (curve 1) also displays a pronounced expansion at very negative s (results not shown).

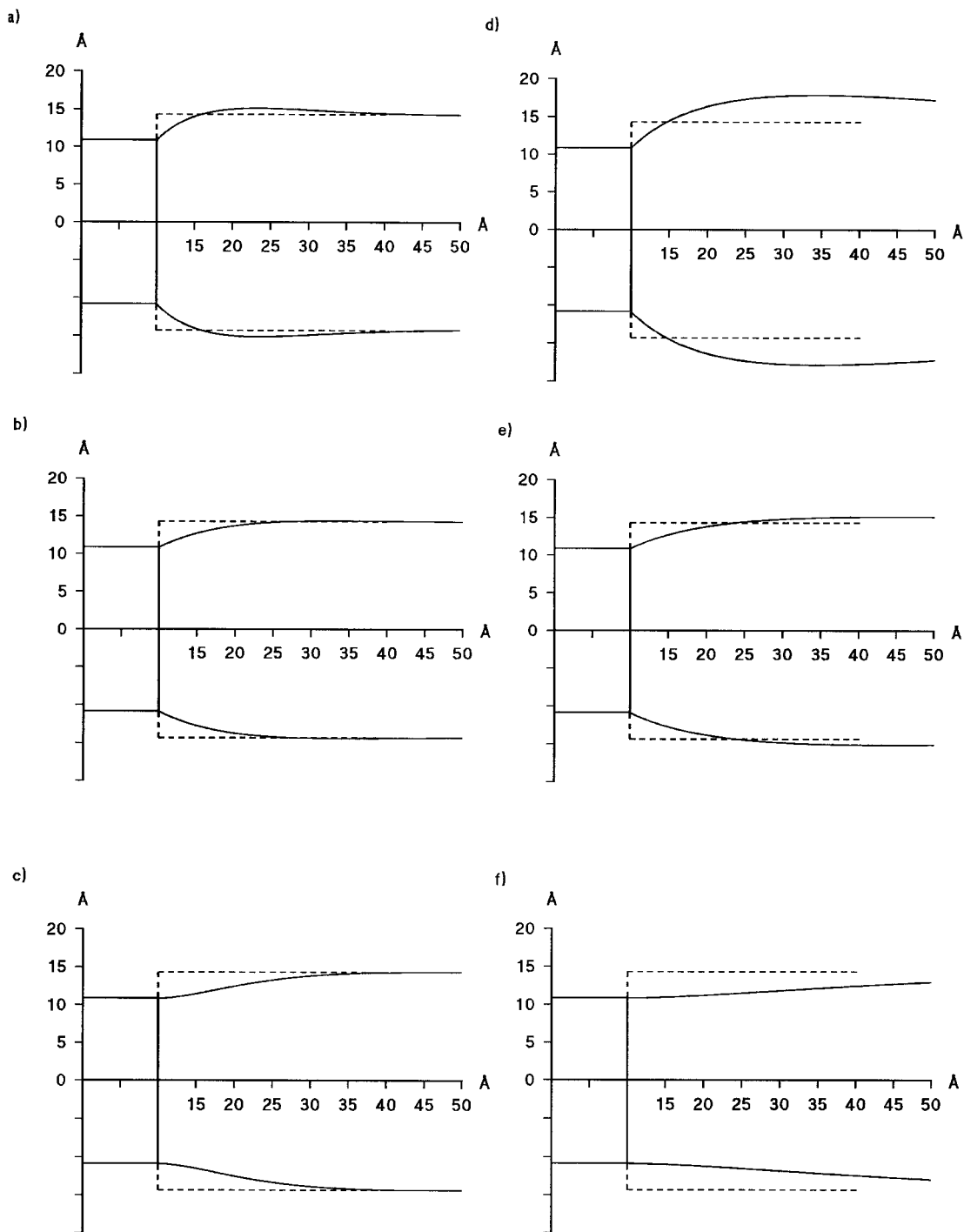


FIGURE 4 Bilayer perturbation profiles for different choices of boundary conditions and material constants. (a–c) Profiles for the reference membrane and different values of s . (a) $s = -1.00$, (b) $s = -0.50$, and (c) $s = 0.00$. (d–f) Profiles for a soft bilayer $K_a = 0.01 K_a^*$ (reference parameters otherwise). (d) $s = -1.00$, (e) $s = -0.50$, and (f) $s = 0.00$.

kT for the reference membrane to 1.33 in the softest bilayer where $K_a = 0.01 K_a^*$. For $s > -0.5$, all curves increase in a sigmoidal manner. At $s = 1$, the value of $\rho_u/\beta^{-1/4}$ is ≈ 2 for all three bilayers, whereas for $s \approx 0$, ρ_u is only slightly larger than $\beta^{-1/4}$ in all cases.

In Fig. 5 b $\rho_{\Delta G}$ is plotted for the same parameters as in Fig. 5 a . The points labeled \star correspond to the s_{\min} values.

For the reference parameter set $\rho_{\Delta G}$ is $\sim 5 \text{ \AA}$ ($= 1/2\beta^{*-1/4}$) independent of the contact slope s . This surprisingly small value of $\rho_{\Delta G}$ shows that most of the deformation energy results from deformations in the first annulus of lipids surrounding the inclusion (see below). This result also emphasizes the importance of the boundary conditions at $r = r_0$. For the softer bilayers (Fig. 5 b , curves 2 and 3), $\rho_{\Delta G}$ is

TABLE 3 Absolute and relative proportions of the energy components for different K_a and s values

K_a/K_a^*	s	$\Delta G_{\text{def}}/kT$	SD/kT	CE/kT	ST/kT	%SD	%CE	%ST
1	-1.00	16.05	12.84	2.41	0.80	80	15	5
	-0.50	4.12	1.28	2.51	0.33	31	61	8
	0.00	11.86	4.03	7.59	0.24	34	64	2
0.1	-1.00	11.52	8.85	1.66	1.01	77	14	9
	-0.50	1.76	1.11	0.32	0.33	63	18	19
	0.00	2.87	1.03	1.66	0.18	36	58	6
0.01	-1.00	8.17	5.56	1.14	1.47	68	14	18
	-0.50	1.35	0.86	0.09	0.39	64	7	29
	0.00	0.83	0.29	0.40	0.14	35	48	17

a nonmonotonic function of s . When $K_a = 0.01 K_a^*$, $\rho_{\Delta G}$ displays a peak close to $s = 0$ (cf. Fig. 4 *f*). Nevertheless, $\rho_{\Delta G}$ is only $\approx \rho_u/2$, and $\rho_{\Delta G}$ is $< \beta^{-1/4}$ for all cases examined.

Radial decomposition of deformation free energy

Depending on the choice of boundary conditions, ΔG_{CE} can be less than, equal to, or larger than ΔG_{SD} . The relative contributions of these two major components to ΔG_{def} vary

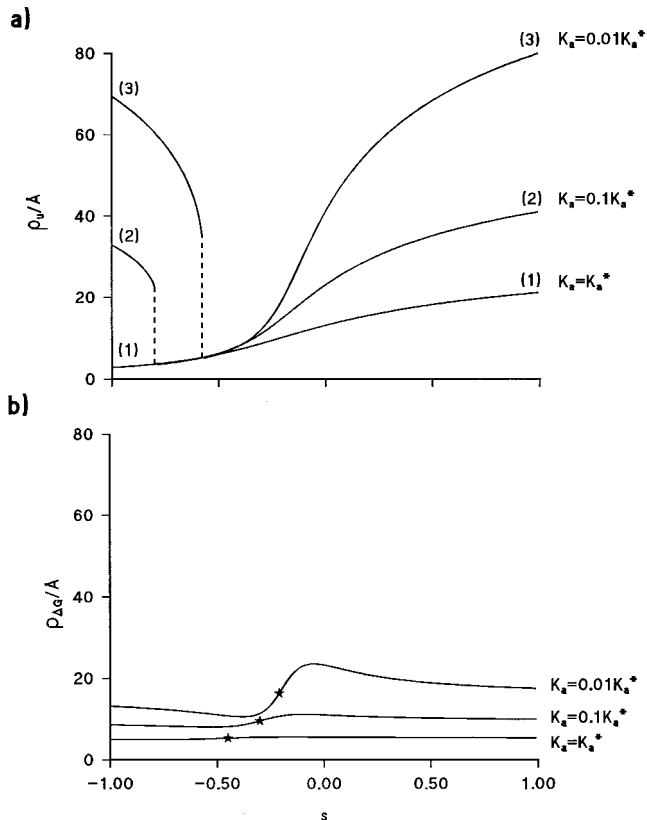


FIGURE 5 Length scales for the bilayer deformations. (a) ρ_u and (b) $\rho_{\Delta G}$ different compression-expansion moduli as functions of s . (1) $K_a = K_a^*$, (2) $K_a = 0.1 K_a^*$, (3) $K_a = 0.01 K_a^*$. Reference parameters otherwise. The corresponding $\beta^{-1/4}$ values are $\approx 11.3 \text{ \AA}$, $\approx 20.1 \text{ \AA}$, and $\approx 35.7 \text{ \AA}$, respectively.

as functions of two parameters, the contact slope s and $\beta^{-1/4}$ (Table 3). This parameter dependence can be further illustrated when the deformation free energy is decomposed radially into the component energy per unit length away from the inclusion (Eq. 16a–c). At both $s = 0$ and $s = s_{\text{min}}$, $\Delta G_{\text{CE}} > \Delta G_{\text{SD}}$ (see Fig. 3 *a*). The radial distribution of the energy, however, shows a more complex behavior (Fig. 6). For $s = 0$, $u_0 = 4 \text{ \AA}$ (Fig. 6 *a*), the splay-distortion component dominates close to the interface but decreases to become nearly zero at 10 \AA ($= \beta^{*-1/4}$), with a marginal contribution at 20 \AA ($\sim 2\beta^{*-1/4}$) from the interface. The compression-expansion component has a maximum at $\sim 2.5 \text{ \AA}$ away from the inclusion and decreases more slowly than the splay-distortion component, thus dominating the deformation energy at distances $> 5 \text{ \AA}$ ($= 1/2 \beta^{*-1/4}$) from the bilayer/inclusion boundary. The surface tension component is negligible (cf. Table 3), and not shown for reasons of clarity. When a minimum energy constraint (Eq. 5d) is imposed on the interface slope (Fig. 6 *b*), the component energies are less, but the splay-distortion energy continues to dominate close to the boundary. The compression-expansion component begins to prevail only at distances of $> 9 \text{ \AA}$ ($= \beta^{*-1/4}$) from the interface. Again the surface tension component is negligible (cf. Table 3).

For the soft bilayer ($K_a = 0.01 K_a^*$) and $s = 0$, the radial distribution of energy components bears qualitative similarities to what is seen for the reference membrane (cf. Fig. 6, *a* and *c*). The splay-distortion component again decreases to nearly zero at $\beta^{-1/4}$ ($\approx 35 \text{ \AA}$), and the compression-expansion component dominates further away from the inclusion, but now a significant surface tension component is present. For the $s = s_{\text{min}}$ solution in the soft bilayer ($K_a = 0.01 K_a^*$) surface tension has become the dominant energy component (Fig. 6 *d*). The splay-distortion component is approximately of the same magnitude, whereas the compression-expansion is negligible. Under selected conditions, ΔG_{ST} may be a major component of the ΔG_{def} .

The linear spring description

In Fig. 2 *b*, the energy versus deformation curve has a parabolic shape, which suggests that ΔG_{def} could be a quadratic function of u . Such a quadratic relationship is a characteristic of simple linear springs and is simple to use in practical applications. It thus becomes important to investigate to what extent a spring approximation is valid. Setting $\bar{u} = u/u_0$ and using Eqs. 5d and e, A11, and A12:

$$\begin{aligned} \Delta G_{\text{def}} &= \frac{K_c}{2} u_0^2 \int_{\Omega} ((\beta_u^{-2} + \nabla^2 \bar{u})^2 + \gamma |\bar{\nabla} \bar{u}|^2) d\Omega \\ &= K_c \pi r_0 u_0^2 \left(-\frac{\partial \bar{u}}{\partial r} \nabla^2 \bar{u} + \bar{u} \frac{\partial}{\partial r} \nabla^2 \bar{u} - \gamma \bar{u} \frac{\partial \bar{u}}{\partial r} \right) \Big|_{r=r_0}. \end{aligned} \quad (20)$$

This has the implication that for either $(\partial/\partial r)\nabla^2 u|_{r_0} = 0$ or $(\partial u/\partial r)|_{r_0} = 0$ the terms in the brackets are independent of

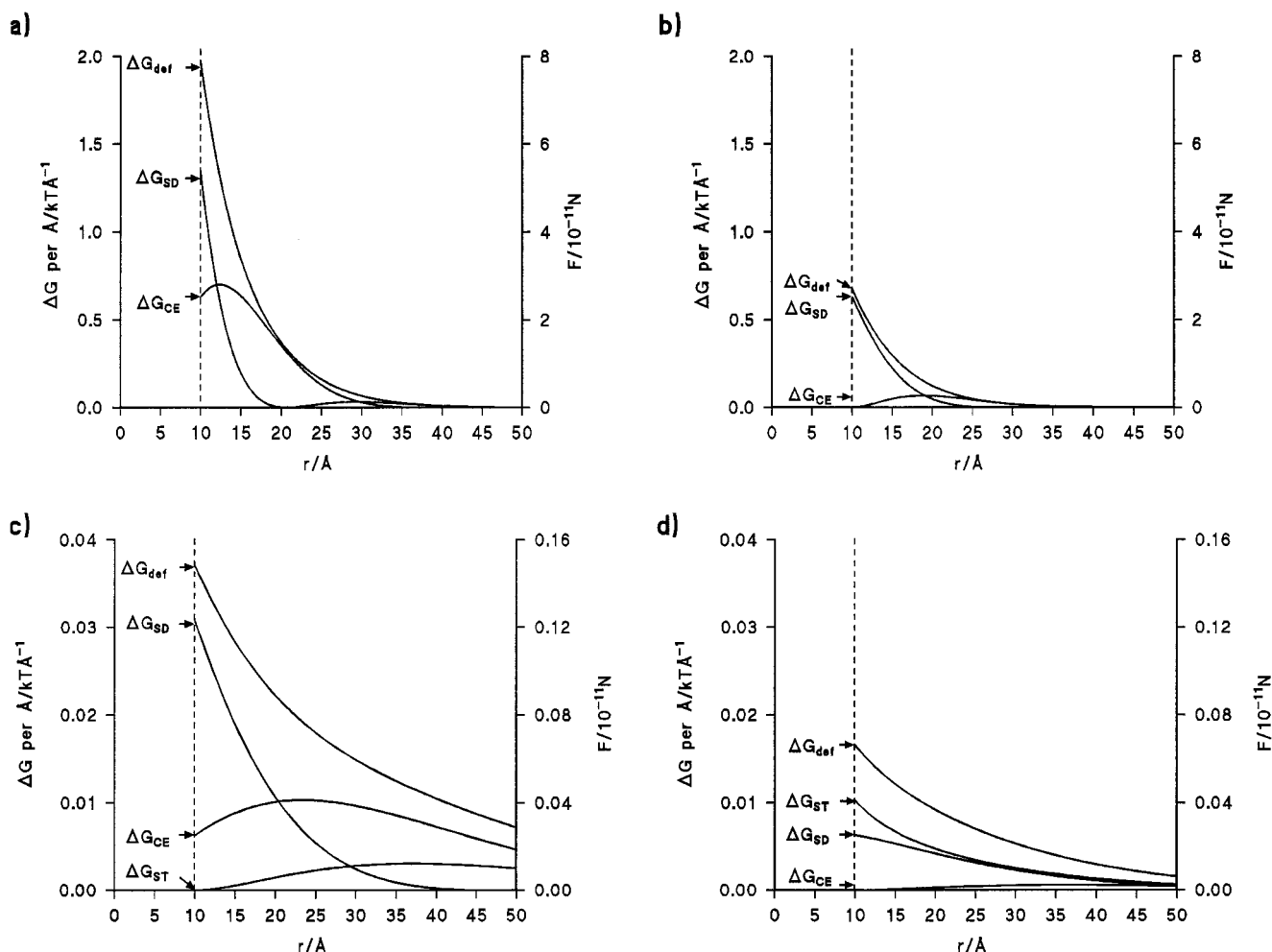


FIGURE 6 Radial decomposition of the deformation energy. (a) The ΔG_{def} components as a function of distance from bilayer/inclusion boundary for $s = 0$ and $u_0 = 4 \text{ \AA}$ (standard parameter set otherwise). The free energy per unit length for the total energy and for each of the components are shown. (b) Same as in (a), except that the contact slope is allowed to relax to its minimal free energy value ($s = s_{\text{min}}$). (c) Same as in (a), except that $K_a = 0.01 K_a^*$. (d) Same as in (b), except that $K_a = 0.01 K_a^*$.

u_0 and ΔG_{def} (Eq. 20) is a quadratic function of u_0 . Generally, ΔG_{def} is a homogeneous 2nd order function of u_0 and s , i.e., $\Delta G_{\text{def}} = a_1 u_0^2 + a_2 s^2 + a_3 u_0 s$ for constants a_1, a_2, a_3 .

The consequences of this are illustrated in Fig. 7. Fig. 7, *a-c* shows results for $s = 0$; Fig. 7, *d-f* shows results for $s = s_{\text{min}}$. Fig. 7, *a* and *d* show the quadratic relationship between ΔG_{def} and u_0 for different values of K_a . Fig. 7, *b* and *c* and *e-f* shows the phenomenological spring constants H ($\Delta G_{\text{def}} = H u_0^2$)⁵ calculated for $s = 0$ (Fig. 7, *b* and *c*) and $s = s_{\text{min}}$ (Fig. 7, *e* and *f*) for the same range of compression-expansion moduli K_a and splay-distortion moduli K_c . Empirically, the results are well described by power laws: $H \sim K_c^\mu$ for fixed K_a , and $H \sim K_a^\nu$ for fixed K_c . Table 4 summarizes values for μ and ν for both boundary conditions: $s =$

0 and $s = s_{\text{min}}$. In either situation we find that $\mu + \nu \approx 1$ (the physical basis for this relation is not clear). Hence

$$\Delta G_{\text{def}} = H u_0^2 \sim K_a \xi^{2\mu} = K_c \xi^{-2\nu} \quad (21)$$

H (and thus ΔG_{def}) also scales with the inclusion radius (Fig. 8 and Table 5). For $s = s_{\text{min}}$ (Fig. 8 *a*), $H \sim r_0^\delta$, where $\delta = 0.976$. The relative energy contributions do not vary with increasing r_0 , but s_{min} changes from -0.4466 ($r_0 = 10 \text{ \AA}$) to -0.3288 for $r_0 = 50 \text{ \AA}$ (Fig. 8 *b*). For $s = 0$ (Fig. 8 *c*) $H \sim r_0^\delta$, where $\delta = 0.815$. In this case the relative energy contributions change slightly with increasing r_0 : the relative CE/SD/ST contributions (in %) varies between 64/34/2 for $r_0 = 10 \text{ \AA}$ and 71/27/2 for $r_0 = 50 \text{ \AA}$ (see Table 5). An increase in r_0 also changes the characteristic lengths, i.e., the $\rho_u(s)$ and $\rho_{\Delta G}(s)$ curves in Fig. 5. For $r_0 = 30 \text{ \AA}$ the shape of the curves are preserved but they are shifted $\sim +0.1 s$ units. For $s = -0.5$ and $s = 0$ the differences in ρ values at $r_0 = 30 \text{ \AA}$ and $r_0 = 10 \text{ \AA}$ amount to $<10\%$ (results not shown).

⁵For integral membrane proteins it may be more convenient to use the total deformation rather than u_0 . If that convention is used $\Delta G_{\text{def}} = (H/4)(d_0 - l)^2$ (cf. Eq. 5c), i.e., the appropriate spring constant will be four times less.

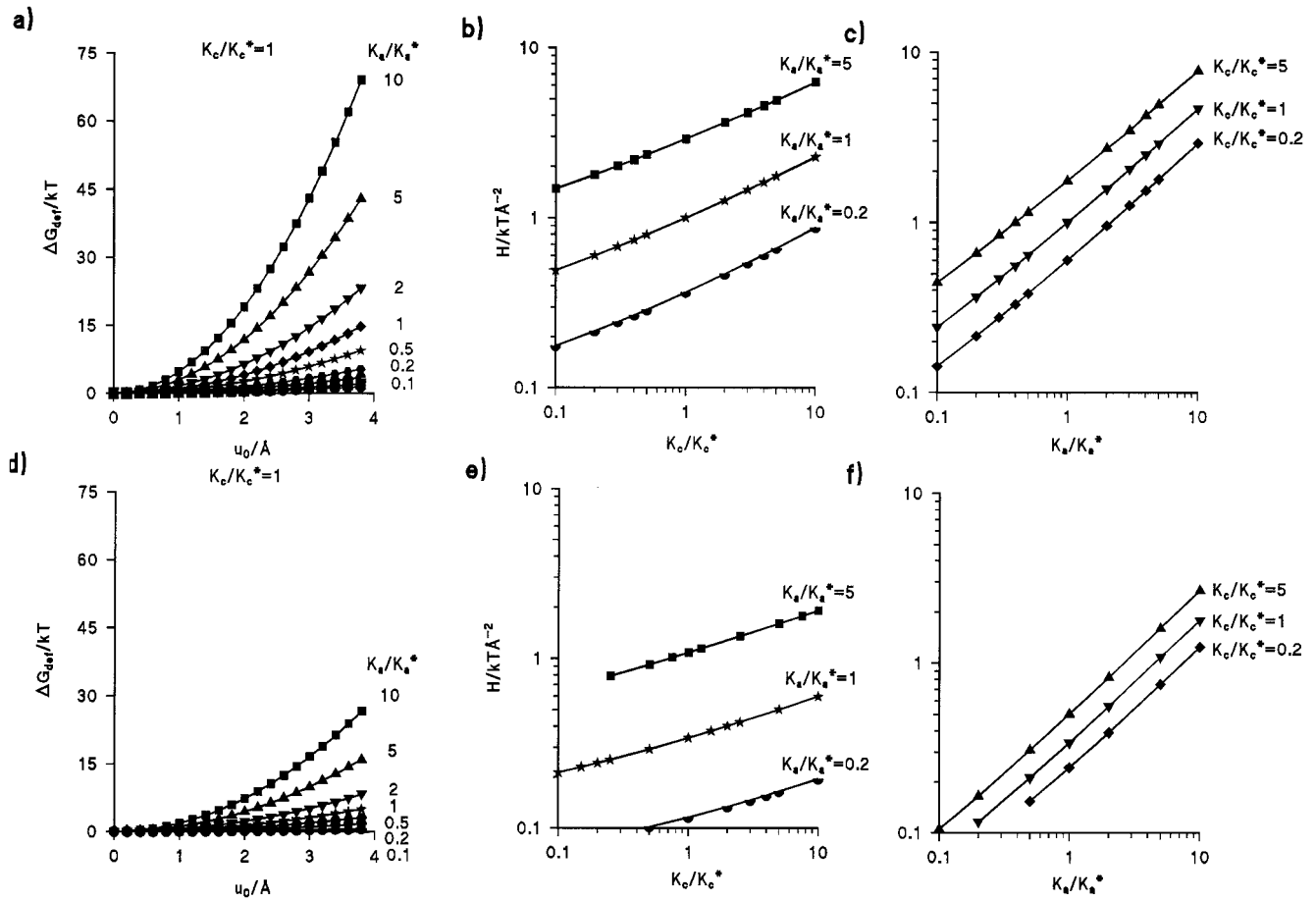


FIGURE 7 The phenomenological spring model. (a) ΔG_{def} when $s = 0$ as a function of u_0 for different values of the compression-expansion modulus relative to K_a^* . Standard parameter set. The points denote the calculated ΔG_{def} values as a function of u_0 . The curves are nonlinear least-squares fits to a linear spring model. $\Delta G = Hu_0^2$ (the correlation coefficient $r = 1.000$ in all cases). (b and c) The phenomenological spring constant H plotted as a function of K_c/K_c^* and K_a/K_a^* . The points denote calculated energy values and the curves are nonlinear least-squares fits to power laws $\Delta H \sim (K_c/K_c^*)^\mu$ or $H \sim (K_a/K_a^*)^\nu$ (the correlation coefficient $r > 0.996$ in all cases). (d-f): Same as in (a-c) but for $s = s_{\text{min}}$ (the correlation coefficient $r > 0.997$ in all cases). μ, ν values are listed in Table 4.

Interdependence between energy components

One might expect that a specific energy component associated with a bilayer deformation should be completely described by the associated mechanical modulus. This is not the case, as already could be inferred from the results in Figs. 4 and 5. Given the importance of this issue, it is further examined in Fig. 9. The results are summarized in Table 6.

Fig. 9 a shows ΔG_{CE} as a function of K_c/K_c^* for $s = 0$. For a constant K_a , a variation in K_c will affect the magnitude of ΔG_{CE} . Similarly, a variation in K_a will affect the magnitude of ΔG_{SD} (Fig. 9 b). In both cases the functional relations can be described by power laws (see Table 6). When $s = s_{\text{min}}$,

these relations are preserved (Fig. 9 c and d), but with a decreased sensitivity of ΔG_{CE} to variations in K_c and an increased sensitivity of ΔG_{SD} to variations in K_a (see Table 6). As for ΔG_{def} , μ and ν depend upon the boundary conditions, but for each energy component $\mu + \nu \approx 1$. Hence

$$\Delta G_{\text{SD}} \sim K_a \xi^{2\mu} = K_c \xi^{-2\nu} \quad (22)$$

$$\Delta G_{\text{CE}} \sim K_a \xi^{2\mu} = K_c \xi^{-2\nu}. \quad (23)$$

DISCUSSION

In this study we provide an analysis of the energetic consequences of an inclusion-induced membrane deformation using a continuum theory of smectic liquid-crystal deformations as applied to lipid vesicle shapes (Helfrich, 1973), which was extended to inclusion-induced deformations by Huang (1986). We note that perturbations in the bilayer thickness μ are expected to decay over a length scale that is

TABLE 4 Scaling parameters for ΔG_{def}

s	μ	ν	$\mu + \nu$
$s = 0$	0.334	0.667	1.001
$s = s_{\text{min}}$	0.287	0.717	1.004

($\Delta G_{\text{def}} \sim K_c^\mu$; $\Delta G_{\text{def}} \sim K_a^\nu$).

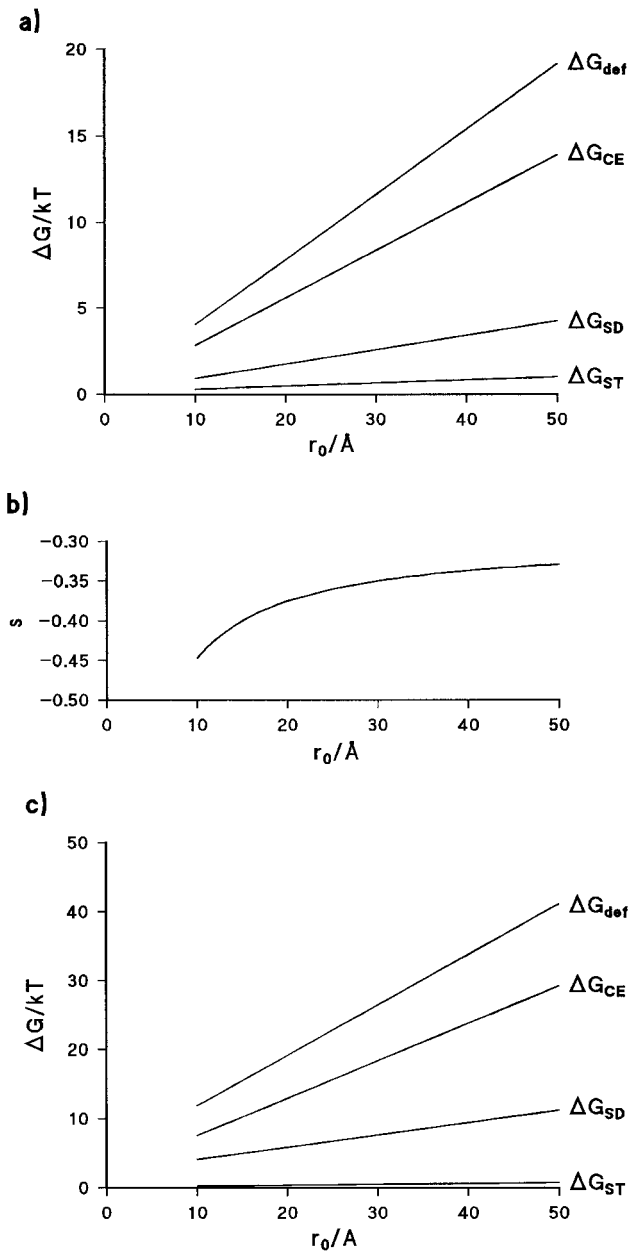


FIGURE 8 The deformation free energy and its components as a function of inclusion radius. (a) Results for $s = s_{\min}$. $\Delta G_{\text{def}} \sim r_0^\delta$, where $\delta = 0.976 \pm 0.001$ (mean \pm SE from least-squares fit). (b): The minimum contact slope as a function of r_0 . (c) Results for $s = 0$, $\delta = 0.815 \pm 0.006$.

of order of the unperturbed thickness d_0 , which is the largest relevant length scale that characterizes a bilayer. Because d_0 is a microscopic length, the continuum elastic description of the bilayer that we employ (Eq. 1) should be viewed as a phenomenological model. The model thus is an approximate description of bilayer deformations at short length scales (and fairly long time scales), which should capture much of the relevant physics. The constants K_a , K_c , and α , as well as the boundary conditions, are fitting parameters: they need not bear a simple relation to the macroscopic quantities that are measured experimentally.

TABLE 5 Effect of inclusion radius on ΔG_{def}

s	$r_0/\text{\AA}$	$\Delta G_{\text{def}}/kT$	$\Delta G_{\text{CE}}/kT$	$\Delta G_{\text{SD}}/kT$	$\Delta G_{\text{ST}}/kT$
$s = 0$	10	4.05	2.83	0.92	0.30
	20	7.81	5.59	1.75	0.48
	30	11.60	8.36	2.58	0.66
	40	15.38	11.13	3.42	0.84
	50	19.18	13.90	4.26	1.01
$s = s_{\min}$	10	11.86	7.54	4.08	0.24
	20	19.12	12.93	5.83	0.36
	30	26.44	18.34	7.62	0.48
	40	33.77	23.76	9.41	0.60
	50	41.11	29.18	11.21	0.72

Boundary conditions

The results of our analysis confirm and extend the findings of Huang (1986) and Helfrich and Jakobsson (1990), as we show that the seemingly contradictory results obtained by these investigators arise simply from their different choices of boundary conditions. In principle, however, these results emerged as solutions to two quite different problems. Huang (1986) used experimental data to determine s and concluded that s is close to zero. Helfrich and Jakobsson used energy minimization to determine s . Both approaches assume perfect hydrophobic coupling between the inclusion and the bilayer hydrophobic core. In both cases Eq. 4 was solved by integrating from the inclusion-bilayer boundary to infinity. The deformation energies, however, differ by roughly a factor of two, the smaller values being obtained by the Helfrich and Jakobsson approach. The $s = 0$ boundary condition is in better accord with experimental results (Huang, 1986), and the apparent failure of the $s = s_{\min}$ boundary condition could arise because the continuum parameters that are used in the model are inappropriate at the short length scales that are of interest here or because there are additional contributions to ΔG_{def} , which are neglected in the model. One such component could be the tilt contribution to the deformation energy (cf. Helfrich, 1973). At the present time, however, there is insufficient information to establish the appropriate choice of boundary conditions at the bilayer/inclusion boundary.

In a somewhat different approach Ring (1996) introduced an apparent relaxation of the hydrophobic coupling in which a non-zero s is taken to imply that the lipids slide outward in a way that maintains strong hydrophobic coupling at the bilayer/inclusion boundary. Under this boundary condition the integration starts from the center of the lipids that surround the inclusion. As expected, the deformation energy in this model is less than that obtained by Huang (1986) or Helfrich and Jakobsson (1990); but the formal development is very similar to that of Helfrich and Jakobsson (1990, see Appendix I).

The lack of experimental information about the nature of the bilayer/inclusion boundary is problematic because the length scales for which the continuum description is applicable are determined by the residual, or time-averaged, "texture" of the microstructure that remains after integrating

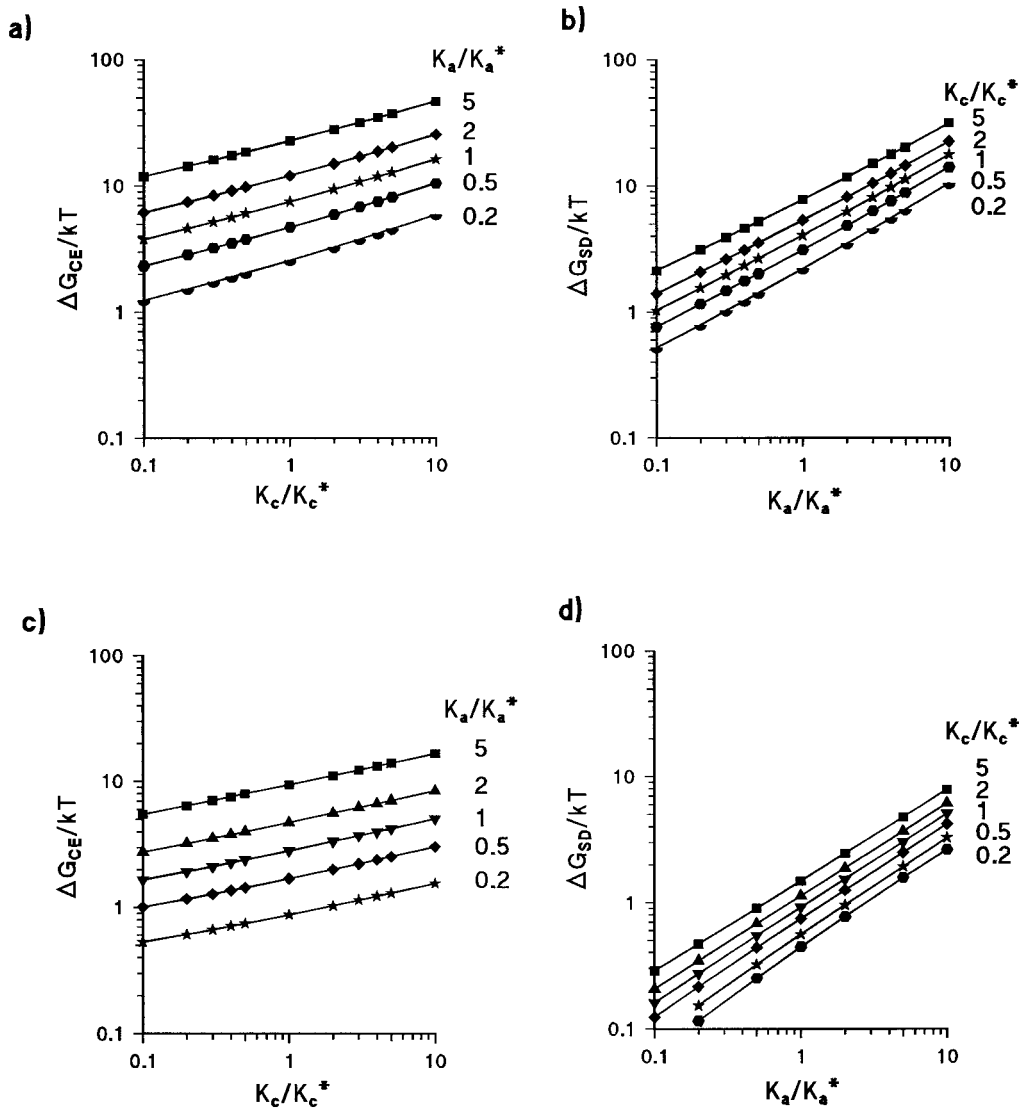


FIGURE 9 Free energy decomposition as a function of K_c/K_c^* and K_a/K_a^* . The points denote calculated energy values and the curves are nonlinear least-squares fits to power laws $\Delta G_{CE} \sim (K_c/K_c^*)^\mu$ or $\Delta G_{SD} \sim (K_a/K_a^*)^\nu$ (the correlation coefficient $r > 0.995$ in all cases). (a and b) $s = 0$; (c and d) $s = s_{\min}$. (a) ΔG_{CE} as function of K_c/K_c^* for different K_a/K_a^* . (b) ΔG_{SD} as function of K_a/K_a^* for different K_c/K_c^* . (c) Same as in (a), but for $s = s_{\min}$. (d) Same as in (b), but for $s = s_{\min}$. (The μ , ν values are listed in Table 6.)

the molecular motions over the relevant time scale. To examine length scales on the order of \AA it is necessary to average the molecular motions over time periods that are of the order of ms (cf. Bloom et al., 1991), which is much longer than the average residence time of a lipid molecule in the inclusion-perturbed bilayer.

TABLE 6 Scaling of energy components

s	Component	μ	ν	$\mu + \nu$
$s = 0$	ΔG_{SD}	0.348	0.638	0.986
	ΔG_{CE}	0.328	0.652	0.980
$s = s_{\min}$	ΔG_{SD}	0.273	0.746	1.019
	ΔG_{CE}	0.244	0.739	0.983

Component $\sim K_c^\mu$; Component $\sim K_a^\nu$.

Energy components and membrane shape

The radial decomposition of the component energies (Fig. 6) show that splay-distortion contribution to ΔG_{def} energy dominates at the bilayer/inclusion interface, whereas the compression-expansion contribution is predominant further away from the inclusion. Any inclusion-induced membrane deformation will thus involve a complex interplay of compression-expansion and splay-distortion of the surrounding bilayer.

Importantly, but not surprisingly, the relative contributions of ΔG_{CE} and ΔG_{SD} to ΔG_{def} are similar. That is, the bilayer deformation energy cannot be attributed solely to either compression-expansion or splay-distortion, which has implications for understanding how the lipid bilayer material properties affect protein function. The bilayer responds

to an imposed distortion by minimizing the overall deformation energy by varying both the CE and SD components, and the effect of this minimization can lead to a large repertoire of shapes (Fig. 4). Taken together with the relative paucity of experimental values for the relevant mechanical moduli in different lipid systems and variation in available values, this complexity has led to the development of simpler approaches that may be used to explain specific cases of protein-lipid interactions.

The linear spring model

In the case of gramicidin channels incorporated in planar lipid bilayers, for example a phenomenological spring model, e.g., the mattress model (Mouritsen and Bloom, 1984), appears to be a useful approximation (Andersen et al., 1992; Durkin et al., 1993; Lundbæk and Andersen, 1994; Lundbæk et al., 1996). In the mattress model the different contributions to the overall deformation free energy are combined and the problem is simplified to the deformation of a linear (Hookean) spring. Somewhat surprisingly, this simplification also applies in the case of systems with energy contributions from both SD and CE components. In the case of contact slope $s = 0$ and $s = s_{\min}$, the spring model constitutes an exact description of the membrane deformation. This considerably simplifies the use of elastic models that include both compression and bending modes, but it does not alleviate the problem of assigning appropriate values to the underlying mechanical moduli.

Parametric interrelations

The separation of energy contributions in our elastic model is problematic. Compression of a monolayer of lipid molecules, for example, would be expected to alter the apparent splay-distortion modulus of the monolayer. K_c and K_a in the formalism presented here, in fact, are not independent descriptors of the mechanical properties of the bilayer in the sense that both reflect the same fundamental parameters that describe lipid-lipid interactions in a monolayer (or bilayer). This dependence is already apparent in the shell model of Evans and Skalak (1980) according to which $K_c = K_a d_0^2$. One modulus therefore renormalizes the other: variations in K_a lead to changes in ΔG_{SD} , and variations in K_c changes ΔG_{CE} . On the other hand, the interpretation of K_c as a true bending modulus has been shown to be valid in H_{II} phase systems, where the work of deformation from this spontaneous radius of curvature is quadratic in curvature and where the associated bending moduli are related to the moduli measured on planar bilayers (Gruner et al., 1986).

The surface tension component of the total deformation free energy, as formulated in Eq. 1, constitutes a negligible part of the total deformation free energy in the solvent-free membrane that is our reference system. If bilayer softness is increased by two orders of magnitude, a substantial part of

the free energy of deformation will be due to surface tension. Thus, for thicker and softer (solvent-containing) bilayers, surface tension could be a significant energy contribution to the total deformation free energy.

Scaling properties

For the chosen reference parameter set, the length scale of the bilayer perturbation ρ_u (Fig. 5 a) depends on boundary conditions (the contact slope s). The corresponding scale property for the total deformation free energy $\rho_{\Delta G}$ is fairly independent of s (Fig. 5 b).

Roughly two-thirds of the total deformation free energy is due to the bilayer deformation within the first annulus of lipid molecules surrounding the inclusion. With increasing softness both length scales become more sensitive to changes in s (Fig. 5, a and b, curves 2 and 3). A relative decrease in the compression-expansion modulus will increase ξ , but ρ_u and $\rho_{\Delta G}$ scale differently. For example, in the case of $s \approx 0$ and $K_a = 0.01 K_a^*$ the maximal $\rho_{\Delta G}$ is just about half of ρ_u , the former being comparable to $2\beta^{*-1/4}$. The different scaling is a reflection of the manner in which the bilayer adapts to the inclusion induced perturbation. The system can tolerate long-range perturbations (meaning $\beta^{*-1/4} \gg d_0$) as far as they are associated with a minimal energy cost. An increase in inclusion radius will increase the energies (ΔG_{def} , ΔG_{CE} , ΔG_{SD} , and ΔG_{ST}), but the increase is a sublinear function of inclusion radius.

Biological implications

Implicit in the elastic membrane model is that there may be a significant energetic penalty associated with even a modest degree of hydrophobic coupling between an integral membrane protein and its host bilayer. Integral membrane protein function may be influenced by the host bilayer if the hydrophobic interface between protein and bilayer is altered as a result of protein activity, e.g., a conformational change associated with an closed \rightleftharpoons open transition in ion channels. Quarternary conformational changes have been described for the nicotinic acetylcholine receptor and gap junction channels (Unwin et al., 1989; Unwin and Ennis, 1984). For gap junction channels ($r_0 = 30 \text{ \AA}$) the open \rightleftharpoons close transition involves a change in the membrane spanning part of the channel, which results in a change in the hydrophobic length of the channel from 30 \AA to 29.7 \AA . If the channel is embedded in a bilayer with a thickness of 30 \AA (perfect hydrophobic match), and with $s = 0$, an open \rightleftharpoons close transition would result in a rather modest ΔG_{def} of 0.22 kT (corresponding to a 25% change in the Boltzmann equilibrium distribution between the open and closed states). For a bilayer thickness of 31 \AA (and $s = 0$), ΔG_{def} would be 2.3 kT (corresponding to a 10-fold change in Boltzmann fac-

tor).⁶ The deformation energies can be larger if the spontaneous monolayer curvature is different from zero (Nielsen, Goulian, and Andersen, unpublished observations).

The deformation profiles obtained using the elastic membrane model marks the average hydrocarbon/headgroup boundary. Thermal motion of the lipids perpendicular to the bilayer will cause changes in thickness (Wiener and White, 1992). The implications of such thermal fluctuations in the instantaneous thickness may in their own right affect properties, but these effects are difficult to determine because the thickness changes depend on sample hydration levels and lipid type.

Relatively modest changes in bilayer properties can change ΔG_{def} by 10–15 kJ/mol (Lundbæk et al., 1996, 1997), corresponding to 4–6 kT per molecule, indicating that the bilayer deformation energy may be of sufficient magnitude to affect protein function. In addition, even though the deformation extends ≈ 30 Å from the inclusion, most deformation arises in the region corresponding to the annulus of lipid molecules that are in intermediate contact with the inclusion. This implies that one should be able to effect substantial changes in the bilayer deformation energy by rather modest changes in the composition of this boundary layer, which could have implications for understanding how lipid-soluble, or amphipathic, substances affect the conformational preference of (and function) of integral membrane proteins. Conversely, the configuration of the hydrocarbon chains in the boundary layer is affected by the inclusion, the result being a (transient) lateral phase separation. Such a separation will change the lipid density around an inclusion and could trigger protein activity as noted earlier by Sackmann (1984).

In conclusion, the present results extend previous work on the coupling between the membrane elastic deformations and protein function (cf. Mouritsen and Bloom, 1984; Sackmann, 1984; Gruner, 1991; Brown, 1994), and provide a rationale for why the function of integral proteins is affected by maneuvers that primarily affect either bilayer thickness (Caffrey and Feigenson, 1981; Johannsson et al., 1981; Criado et al., 1984) or propensity to form nonbilayer phases (Navarro et al., 1984; Brown, 1994; McCallum and Epan, 1995). In either case, the manipulations of the bilayer environment alter ΔG_{def} , which in turn can affect the equilibrium distribution between different protein conformations (Andersen et al., 1992; Gruner, 1991; Lundbæk et al., 1997).

APPENDIX I

In the boundary conditions considered throughout the paper ($s = s_{\text{min}}$ and $s = 0$) there is strong hydrophobic coupling between the inclusion and the immediately surrounding lipid molecules. If this condition is relaxed and

the lipid molecules at the inclusion hydrophobic surface are allowed to “slide” outward (away from the bilayer symmetry plane), the overall bilayer deformation will be less.

This is formulated in a set of boundary condition suggested by Ring (1996) (see Fig. A1, *a* and *b*). In this model s is defined by energy minimization but the lipid molecules closest to the inclusion are displaced in a direction parallel to the z axis of the symmetry axis of the inclusion, which reduces the contribution of acyl chain compression of the nearest-neighbor lipids. The actual displacement $r_2 \sin(\theta)$ is supposed to be determined by factors such as the balance of forces between headgroups and hydrophobic repulsion of the hydrocarbon-water contact, and is assumed to be of the same order as the lipid-lipid separation (Ring, 1996). The formal difference between the $s = s_{\text{min}}$ condition and this “relaxed” condition, referred to in the following as the $s = s'_{\text{min}}$ boundary condition, is that $u(r'_0) = u_0 + r_2 \sin(\theta)$, where $r'_0 = r_1 + r_2 \cos(\theta)$. In Fig. 1 *a* $s = \tan(\theta) < 0$, so $u(r'_0) \leq u(r_0)$ and $r'_0 \geq r_0$. For $r_1 = 10$ Å $r_2 = 0$ Å, the two sets of conditions are identical. Fig. A1 *a* shows the situation where $r_1 = 7$ Å and $r_2 = 3$ Å (Ring, 1996), whereas in Fig. A1 *b* $r_1 = 10$ Å and $r_2 = 4.5$ Å.

Under these conditions the bilayer deformation energy will be less than for $s = s_{\text{min}}$ [see Fig. A1 *c* (curve labeled $s = s'_{\text{min}}$)]. When the curve is replotted [arrow (1) in Fig. A1 *c*] as a function of the “actual” deformation $u(r'_0) = u_0 + r_2 \sin(\theta)$, however, the resulting relaxed minimum solution is virtually identical to the $s = s_{\text{min}}$ solution. This is due to the fact that for $r_1 = 7$ Å and $r_2 = 3$ Å, $r_0 \approx r'_0$, so the difference is primarily due to a change in the effective u at the interface. The solution given by Ring (1996) can thus be obtained from the $s = s_{\text{min}}$ by simple scaling of u . The distances $r_1 = 7$ Å and $r_2 = 3$ Å are too low, however, to account for a gramicidin channel incorporated in a phospholipid bilayer. $r_1 = 10$ Å and $r_2 = 4.5$ Å might be more appropriate. For these parameters the energies, when plotted as function of u_0 , are less than for $s = s_{\text{min}}$, even though the effective inclusion radius r_1 is larger than r_0 (Fig. A1 *b*), $u(r'_0)$ is less than u_0 , the result being overall less deformation. Again this curve can be plotted as a function of the actual deformation, $u(r'_0)$ [arrow (2) in Fig. A1 *c*] resulting in a steeper curve than for the $s = s_{\text{min}}$ situation. But when the $s = s_{\text{min}}$ curves are scaled using the power law for inclusion radius illustrated in Fig. 8 [arrow (3) in Fig. A1 *c*], these two solutions become almost identical. That is, solutions obtained by the $r_1 = 10$ Å, $r_2 = 4.5$ Å boundary condition can also be found by appropriate scaling of the $s = s_{\text{min}}$ solution.

It should be noted that the interpretation of r_0 and r'_0 is different. For r_0 , as the lower boundary for the energy integral in Eq. 1, the integration includes the total cross-sectional area of each of the lipid molecules in the first annulus surrounding the inclusion (Fig. 1, *b* and *c*), whereas for r'_0 the integration includes only half of the cross-sectional area for each of the lipids in the first surrounding annulus (Fig. A1, *a* and *b*).

APPENDIX II

For physically acceptable deformation profiles the solutions to Eq. 6 must be real-valued continuous functions of bounded variation in any interval $[a, b]$, $0 < a < b < +\infty$. Assuming radial symmetry (cylindrical coordinates) and

$$\int_0^{+\infty} \sqrt{r} |u(r)| dr \quad (\text{A1})$$

is finite, which should pose no restrictions on the solution, u can be expressed using Hankel’s integral theorem (Lebedev et al., 1979):

$$\begin{aligned} u(z) &= \int_0^{\infty} \mathcal{T}_0(kz) k \left(\int_0^{\infty} u(\sigma) \mathcal{T}_0(k\zeta) d\zeta \right) dk \\ &= \int_0^{\infty} \mathcal{T}_0(kz) A(k) dk \end{aligned} \quad (\text{A2})$$

⁶These estimates for the membrane deformations energy were obtained using values for K_a and K_c in SOPC bilayers with 50 mol % cholesterol: a situation we believe describes biological membranes better than the reference values used in previous studies (see Table 1).

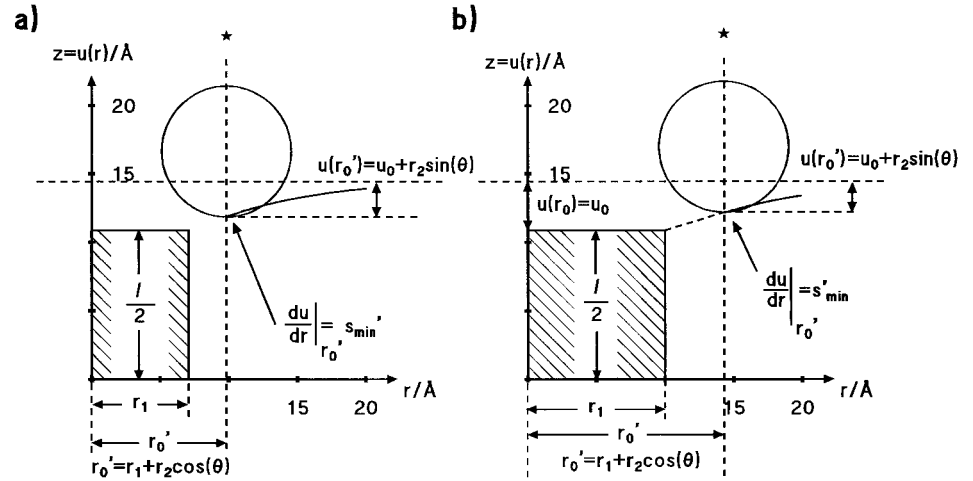
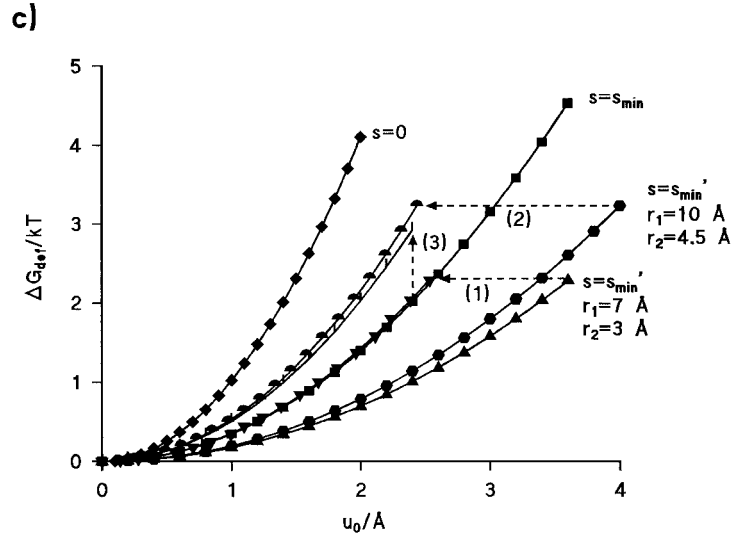


FIGURE A1 See Appendix 1 for details.



where the integral in the parenthesis is the Hankel transform of u and \mathcal{T}_0 is the zero-order Bessel function of the first kind (Abramowitz and Stegun, 1968).

The solutions of the quadratic expression Eq. 6 can be obtained as solutions of the equation

$$\nabla^2 u = \eta u \tag{A3}$$

where

$$\eta = \frac{1}{2} \left(\frac{\gamma}{d_0} \pm \sqrt{\left(\frac{\gamma}{d_0} \right)^2 - \left(\frac{2}{\xi d_0} \right)^2} \right) \quad \gamma = \alpha/K_c, \quad \xi = \sqrt{\frac{K_c}{K_a}} \tag{A4}$$

For any argument z

$$-\nabla^2 \mathcal{T}_0(kz) = k^2 \mathcal{T}_0(kz). \tag{A5}$$

and Eq. A2 can be used to solve Eq. A3. This leads to

$$-(k^2 + \eta)A(k) = 0 \Rightarrow u(z) = A_1 \mathcal{T}_0(i\sqrt{\eta}z) + A_2 \mathcal{T}_0(-i\sqrt{\eta}z) \tag{A6}$$

The solutions are real-valued functions, $u^*(z) = u(z)$, and $u(z)$ can be written as

$$\begin{aligned} u(z) &= A[\mathcal{T}_0(i\sqrt{\eta}z) + \mathcal{T}_0(-i\sqrt{\eta}z)] \\ &= A[\mathcal{I}_0(\sqrt{\eta}z) + \mathcal{I}_0(-\sqrt{\eta}z)] \end{aligned} \tag{A7}$$

where \mathcal{I}_0 is the modified zero-order Bessel function of the first kind (Abramowitz and Stegun, 1968). For vanishingly small α , $u(r)$ has the form $f(r/\sqrt{\xi d_0})$ and using Eq. A4 and Eq. 7 we have $\beta^{-1/4} = \sqrt{\xi d_0}$ as a characterizing length scale for the problem.

The solutions must satisfy the constraint of asymptotic convergency

$$\lim_{r \rightarrow \infty} u(r) = 0 \tag{A8}$$

The modified zero-order Bessel functions of the first kind are divergent, so to get the desired solution we expand in terms of zero-order Bessel functions of the second kind \mathcal{Y}_0 (Abramowitz and Stegun, 1968).

$$\mathcal{Y}_0(iz) = i\mathcal{I}_0(z) - \frac{2}{\pi} \mathcal{K}_0(z), \quad -\pi < \arg(z) \leq \pi/2 \tag{A9}$$

and a constrained solution to Eq. 6 can be constructed as

$$u(z) = A[\mathcal{Y}_0(i\sqrt{\eta}z) + \mathcal{Y}_0(-i\sqrt{\eta}z)] \sim \mathcal{H}_0(\sqrt{\eta}z) \quad (\text{A10})$$

where \mathcal{H}_0 is the modified first-order Bessel function of the first kind (Abramowitz and Stegun, 1968).

Using Eq. 7, the expression for the energy (Eq. 1) is given by

$$\begin{aligned} \Delta G_{\text{def}} &= \int_{\Omega} \frac{1}{2} \left[\frac{K_a}{d_0^2} u^2 + K_c (\nabla^2 u)^2 + \alpha |\tilde{\nabla} u|^2 \right] d\Omega \\ &= \frac{K_c}{2} \int_{\Omega} \left((\nabla^2 u)^2 + \beta u^2 + \gamma |\tilde{\nabla} u|^2 \right) d\Omega. \quad (\text{A11}) \end{aligned}$$

This surface integral can be expressed as a contour integral around the inclusion bilayer boundary ω (Landau and Lifschitz, 1986, p. 40):

$$\begin{aligned} \Delta G_{\text{def}} &= \frac{K_c}{2} \oint_{\omega} \left((\tilde{n} \cdot \tilde{\nabla} u) \nabla^2 u - u (\tilde{n} \cdot \tilde{\nabla} \nabla^2 u) + \gamma u (\tilde{n} \cdot \tilde{\nabla} u) \right) d\omega \\ &= K_c \pi r_0 \left(-\frac{\partial u}{\partial r} \nabla^2 u + u \frac{\partial}{\partial r} \nabla^2 u - \gamma u \frac{\partial u}{\partial r} \right) \Big|_{r=r_0} \\ &= K_c \pi r_0 \left(-s \nabla^2 u \Big|_{r=r_0} + u_0 \frac{\partial}{\partial r} \nabla^2 u \Big|_{r=r_0} - \gamma u_{0s} \right) \quad (\text{A12}) \end{aligned}$$

Using Eqs. 8 and 10a and b,

$$\nabla^2 u \Big|_{r=r_0} = A_+ k_+^2 \mathcal{H}_0(k_+ r) + A_- k_-^2 \mathcal{H}_0(k_- r) \quad (\text{A13})$$

$$\frac{\partial}{\partial r} \nabla^2 u \Big|_{r=r_0} = A_+ k_+^3 \mathcal{H}'_0(k_+ r) + A_- k_-^3 \mathcal{H}'_0(k_- r) \quad (\text{A14})$$

Substituting A13 and 14 into A12 gives the result (Eq. 13).

We thank J. A. Lundbæk for helpful discussions.

The work described in this paper was supported by National Institutes of Health Grant GM21342 (to O.S.A.) and the Danish Natural Science Research Council SNF Grant 11-1219-1 (to C.N.). C.N. is a N. & R. Winston Fellow and M.G. is a W. M. Keck Fellow.

REFERENCES

- Abney, J. R., and J. C. Owicki. 1985. Theories of protein-lipid and protein-protein interactions in membranes. In *Progress in Protein-lipid Interactions*. A. Watts and J. DePont, editors. Elsevier, New York.
- Abramowitz, M., and I. Stegun. 1968. *Handbook of Mathematical Functions*. Dover Publications, New York.
- Alvarez, O., and R. Latorre. 1978. Voltage-dependent capacitance in lipid bilayers made from monolayers. *Biophys. J.* 21:1-17.
- Andersen, O. S., D. B. Saywer, and R. E. Koeppe II. 1992. Modulation of channel function by the host bilayer. In *Biomembrane Structure & Function—The State of the Art*. B. P. Garber and K. R. K. Earswaran, editors. Adenine Press, 227-243.
- Baldwin, P. A., and W. L. Hubbell. 1985. Effects of lipid environment on the light-induced conformational changes of rhodopsin. 2. Roles of lipid chain length, unsaturation, and phase state. *Biochemistry*. 24: 2633-2639.
- Bienvenüe, A., and J. S. Marie. 1994. Modulation of protein function by lipids. *Curr. Top. Membr.* 40:319-354.
- Bloom, M., E. Evans, and O. G. Mouritsen. 1991. Physical properties of the fluid lipid-bilayer component of cell membranes: a perspective. *Q. Rev. Biophys.* 24:293-397.
- Brochard, F., de Gennes, P.-G., and P. Pfeuty. 1976. Surface tension and deformations of membranes structures: relation to two-dimensional phase transitions. *J. Physique*. 37:1099-1104.
- Brochard, F., and J.-F. Lennon. 1975. Frequency spectrum of the flicker phenomenon in erythrocytes. *J. Physique*. 36:1035-1047.
- Brown, M. F. 1994. Modulation of rhodopsin function by properties of the membrane bilayer. *Chem. Phys. Lipids*. 73:159-180.
- Caffrey, M., and G. W. Feigenson. 1981. Fluorescence quenching in model membranes. 3. Relationship between calcium adenosinetriphosphatase enzyme activity and the affinity of the proteins for phosphatidylcholines with different acyl chain characteristics. *Biochemistry*. 20:1949-1961.
- Canham, P. B. 1970. The minimum energy of bending as a possible explanation of the biconcave shape of the human red blood cell. *J. Theor. Biol.* 26:61-81.
- Criado, M., H. Eibl, and F. J. Barrantes. 1984. Functional properties of the acetylcholine receptor incorporated in model lipid membranes. *J. Biol. Chem.* 259:9188-9198.
- Dan, N., A. Berman, P. Pincus, and S. A. Safran. 1994. Membrane-induced interactions between inclusions. *J. Phys. II France*. 4:1713-1725.
- Dan, N., P. Pincus, and S. A. Safran. 1993. Membrane-induced interactions between inclusions. *Langmuir*. 9:2768-2771.
- de Gennes, P. G. 1974. *The Physics of Liquid Crystals*. Clarendon Press, Oxford.
- Devaux, P. F., and M. Seigneuret. 1985. Specificity of lipid-protein interactions as determined by spectroscopic techniques. *Biochim. Biophys. Acta*. 822:63-125.
- Durkin, J. T., L. L. Providence, R. E. Koeppe, and O. S. Andersen. 1993. Energetics of heterodimer formation among gramicidin analogs with an NH₂-terminal addition or deletion. *J. Mol. Biol.* 231:1102-1121.
- Elliott, J. R., and D. A. Haydon. 1979. The interaction of *n*-octanol with black lipid bilayer membranes. *Biochim. Biophys. Acta*. 557:259-263.
- Elliott, J. R., D. Needham, J. P. Dilger, O. Brandt, and D. A. Haydon. 1985. A quantitative explanation of the effect of some alcohols on gramicidin single-channel lifetime. *Biochim. Biophys. Acta*. 814: 401-404.
- Elliott, J. R., D. Needham, J. P. Dilger, and D. A. Haydon. 1983. The effects of bilayer thickness and tension on gramicidin single-channel lifetime. *Biochim. Biophys. Acta*. 735:95-103.
- Engelhart, H., H. P. Duwe, and E. Sackman. 1985. Bilayer bending elasticity measured by Fourier analysis of thermally excited surface undulations of flaccid vesicles. *J. Phys. Lett.* 46:L395-L400.
- Evans, E. A., and R. M. Hochmuth. 1978. Mechanochemical properties of membranes. In *Current Topics in Membranes and Transport*, Vol. 10. F. Bronner and A. Kleinzeller, editors. Academic Press, New York. 1-64.
- Evans, E. A., and D. Needham. 1987. Physical properties of surfactant bilayer membranes: thermal transitions, elasticity, rigidity, cohesion, and colloidal interactions. *J. Phys. Chem.* 19:4219-4228.
- Evans, E., and W. Rawicz. 1990. Entropy-driven tension and bending elasticity in condensed fluid membranes. *Phys. Rev. Lett.* 64: 2094-2097.
- Evans, E., and R. Skalak. 1980. *Mechanics and Thermodynamics of Biomembranes*. CRC Press, Boca Raton, FL.
- Gruner, S. M. 1991. *Biologically Inspired Physics*. L. Peltiy, editor. Plenum Press, New York. 127-135.
- Gruner, S. M., V. A. Parsegian, and R. P. Rand. 1986. Directly measured deformation energy of phospholipid H_{II} hexagonal phases. *Faraday Discuss. Chem. Soc.* 81:29-37.
- Helfrich, W. 1973. Elastic properties of lipid bilayers: theory and possible experiments. *Z. Naturforsch.* 28c:693-703.
- Helfrich, P., and E. Jakobsson. 1990. Calculation of deformation energies and conformation in lipid membranes containing gramicidin channels. *Biophys. J.* 57:1075-1084.
- Hendry, B. M., W. Urban, and D. A. Haydon. 1978. The blockage of the electric conductance in a pore-containing membrane by the *n*-alkanes. *Biochim. Biophys. Acta*. 513:106-116.
- Hladky, S. B., and D. W. R. Gruen. 1982. Thickness fluctuations in black lipid membranes. *Biophys. J.* 38:251-258.

- Huang, H. W. 1986. Deformation free energy of bilayer membrane and its effects on gramicidin channel lifetime. *Biophys. J.* 50:1061–1070.
- Jähnig, F. 1996. What is the surface tension of a lipid-bilayer membrane? *Biophys. J.* 71:1348–1349.
- Johannsson, A., G. A. Smith, and J. C. Metcalfe. 1981. The effect of bilayer thickness on the activity of the $\text{Na}^+ + \text{K}^+$ ATPase. *Biochim. Biophys. Acta.* 641:416–421.
- Landau, L. D., and E. M. Lifshitz. 1986. *Theory of Elasticity—Course of Theoretical Physics*, 3rd ed., Vol. 7. Butterworth-Heinemann, Oxford.
- Lebedev, N. N., I. P. Skalskaya, and Y. S. Uflyand. 1979. *Worked Problems in Applied Mathematics*. Dover Publications, New York.
- Lundbæk, J. A., and O. S. Andersen. 1994. Lysophospholipids modulate channel function by altering the mechanical properties of lipid bilayers. *J. Gen. Physiol.* 104:645–673.
- Lundbæk, J. A., P. Birn, J. Girshman, A. J. Hansen, and O. S. Andersen. 1996. Membrane stiffness and channel function. *Biochemistry.* 35:3825–3830.
- Lundbæk, J. A., A. M. Maer, and O. S. Andersen. 1997. Lipid bilayer electrostatic energy, curvature stress and assembly of gramicidin channels. *Biochemistry.* 36:5695–5701.
- Marcelja, S. 1976. Lipid-mediated protein interaction in membranes. *Biochim. Biophys. Acta.* 455:1–7.
- McCallum, C. D., and R. M. Epand. 1995. Insulin receptor autophosphorylation and signaling is altered by modulation of membrane physical properties. *Biochemistry.* 34:1815–1824.
- Miao, L., U. Seifert, M. Wortis, and H.-G. Döbereiner. 1994. Budding transitions of fluid-bilayer vesicles: the effect of area-difference elasticity. *Phys. Rev. E.* 49:5389–5407.
- Mouritsen, O. G., and M. Bloom. 1984. Mattress model of lipid-protein interactions in membranes. *Biophys. J.* 36:141–153.
- Nagle, F. J. 1980. Theory of the main lipid phase transition. *Annu. Rev. Phys. Chem.* 31:157–195.
- Navarro, J., M. Toivo-Kinnucan, and E. Racker. 1984. Effect of lipid composition on the calcium/adenosine 5'-triphosphate coupling ratio of the Ca^{2+} -ATPase of sarcoplasmic reticulum. *Biochemistry.* 23:130–135.
- Needham, D. 1995. Cohesion and permeability of lipid bilayer vesicles. In *Permeability and Stability of Lipid Bilayers*. E. A. Disalvo and S. A. Simon, editors. CRC Press, Boca Raton, FL. 49–76.
- Needham, D., and R. S. Nunn. 1990. Elastic deformation and failure of lipid bilayer membranes containing cholesterol. *Biophys. J.* 58:997–1009.
- Neher, E., and H. Eibl. 1977. The influence of phospholipid polar groups on gramicidin channels. *Biochim. Biophys. Acta.* 464:37–44.
- Nielsen, C., M. Goulian, and O. S. Andersen. 1997. Energetics of inclusion-induced membrane deformation. *Biophys. J.* 72:190a. (Abstr.).
- Niggemann, G., M. Kummrow, and W. Helfrich. 1995. The bending rigidity of phosphatidylcholine bilayers: dependence on experimental method, sample cell sealing, and temperature. *J. Phys. II France.* 5:413–425.
- Owicky, J. C., and H. M. McConnell. 1979. Theory of protein-lipid and protein-protein interactions in bilayer membranes. *Proc. Natl. Acad. Sci. U.S.A.* 76:4750–4754.
- Owicky, J. C., M. W. Springgate, and H. M. McConnell. 1978. Theoretical study of protein-lipid interactions in bilayer membranes. *Proc. Natl. Acad. Sci. U.S.A.* 75:1616–1619.
- Press, W. H., B. P. Flannery, S. A. Teukolsky, and W. T. Vetterling. 1986. *Numerical Recipes*. Cambridge University Press, Cambridge.
- Requena, J., and D. A. Haydon. 1975. The Lippmann equation and the characterization of black lipid films. *J. Colloid Interface Sci.* 51:315–327.
- Ring, A. 1996. Deformation free energy of bilayer membrane and its effects on gramicidin channel lifetime. *Biochim. Biophys. Acta.* 1278:147–159.
- Sackmann, E. 1984. Physical basis of trigger processes and membrane structures. *Biol. Membr.* 5:105–141.
- Schneider, M. B., J. T. Jenkins, and W. W. Webb. 1984. Thermal fluctuations of large quasi-spherical bimolecular phospholipid vesicles. *J. Physique.* 45:1457–1472.
- Seddon, J. M. 1990. Structure of the inverted hexagonal (H_{II}) phase, and non-lamellar phase transitions. *Biochim. Biophys. Acta.* 1031:1–69.
- Servuss, R. M., W. Harbich, and W. Helfrich. 1976. Measurement of the curvature-elastic modulus of egg lecithin bilayers. *Biochim. Biophys. Acta.* 436:900–903.
- Singer, S. J., and G. L. Nicolson. 1972. The fluid mosaic model of the structure of cell membranes. *Science.* 175:720–731.
- Song, J., and R. E. Waugh. 1993. Bending rigidity of SOPC membranes containing cholesterol. *Biophys. J.* 64:1967–1970.
- Unwin, N. 1989. The structure of ion channels in membranes of excitable cells. *Neuron.* 3:665–676.
- Unwin, P. T. N., and P. D. Ennis. 1984. Two configurations of a channel-forming membrane protein. *Nature.* 307:609–613.
- White, S. H. 1978. Formation of “solvent-free” black lipid bilayer membranes from glyceryl monooleate dispersed in squalene. *Biophys. J.* 23:337–347.
- Wiener, M. C., and S. H. White. 1992. Structure of a fluid dioleoylphosphatidylcholine bilayer determined by joint refinement of x-ray and neutron scattering. *Biophys. J.* 61:434–447.